Desalination 491 (2020) 114564

Contents lists available at ScienceDirect

Desalination

journal homepage: www.elsevier.com/locate/desal

New hydrogel materials for improving solar water evaporation, desalination and wastewater treatment: A review

Swellam W. Sharshir[a,b,c,*], Almoataz M. Algazzar[c], K.A. Elmaadawy[d,h], A.W. Kandeal[a,c], M.R. Elkadeem[e,f], T. Arunkumar[g], Jianfeng Zang[b,**], Nuo Yang[a,*]

[a] State Key Laboratory of Coal Combustion, School of Energy and Power Engineering, Huazhong University of Science and Technology, Wuhan 430074, China
[b] School of Optical and Electronic Information, Huazhong University of Science and Technology, Wuhan 430074, China
[c] Mechanical Engineering Department, Faculty of Engineering, Kafrelsheikh University, Kafrelsheikh 33516, Egypt
[d] School of Environmental Science and Engineering, Huazhong University of Science and Technology (HUST), Wuhan, Hubei 430074, China
[e] School of Electrical and Electronic Engineering, Huazhong University of Science and Technology, Wuhan, China
[f] Electrical Power and Machines Engineering Department, Faculty of Engineering, Tanta University, Tanta 31521, Egypt
[g] School of Chemical Sciences & Technology, Yunnan University, Kunming 650091, China
[h] Civil Engineering Department, Faculty of Engineering, Al-Azhar University, Cairo, Egypt

ARTICLE INFO

Keywords:
Hydrogel
Solar energy
Water evaporation
Desalination
Wastewater remediation

ABSTRACT

Ongoing to the modern societies and global economic developments, the water is recognized as one of the main concerns of humankind, particularly with the continuous decrease of the freshwater supply. Solar energy, which is abundant and available in many areas, can solve the problem of long-term energy and freshwater reduction in the whole world. Researchers do their best to solve this problem in different ways. Currently, many studies have used solar energy to improve the efficiency of evaporation, solar desalination, and wastewater treatment since it is the basis for freshwater. One of the new ways applied to achieve this is named "hydrogel", which has various structures. Hydrogel, as a novel light-absorbing material, is an effective technique to enhance photothermal solar efficiency conversion by decreasing the heat loss in the heat transfer process due to the heat localization on the air-water interface. Moreover, hydrogel has many pores structures with excellent water transport from the bottom to the water-air interface. Hydrogels are floatable, durable, anti-fouling, and suitable recycling materials, which are energetically favorable for harvesting and amplifying the steam generation. Furthermore, over the past three years, they have revolutionized solar water vaporization with an evaporation efficiency of 95% and the evaporation rate of 4 kg/(m^2. hr), which cannot be achieved by other materials.

1. Introduction

Currently, the lack of clean water has become one of the serious global problems that threaten the continuity of humankind and needs to be promptly solved [1,2]. Numerous renewable energies (REs) have been established, such as solar energy (SE), wind energy, geothermal energy, and tidal energy. However, SE is the most abundant RE resources on our planet, due to its availability and inexhaustibility everywhere (see Fig. 1). Energy conversion and clean water production methods based on SE appear to be possible ways to solve current mentioned global challenges, which have been excessively anxious by researchers all over the world [3,4]. SE is used in many fields such as photochemical fields [5], photothermal fields [6], solar photovoltaic cells [7] water heating [8], air heating [9], drying applications [10], and so on.

Furthermore, water desalination driven by SE introduces a suitable solution for freshwater scarcity in remote and arid regions. Conventional types of solar desalination, such as solar still, have small conversion energy efficiency because of the large amount of heat needed to raise bulk water temperature before its being evaporated [11]. Nowadays, there are many efficient technologies in the field of desalination such as reverse osmosis (RO) [12], multi-effect desalination (MED) [13], thermal vapor compression (TVC) [14], humidification and dehumidification (HDH) [15,16], hybrid system [17–19] and multistage flash (MSF) [20]. In the beginning, MED, TVC, and MSF were the most common desalination technologies, but RO has become

* Corresponding authors at: State Key Laboratory of Coal Combustion, School of Energy and Power Engineering, Huazhong University of Science and Technology, Wuhan 430074, China.
** Corresponding author at: School of Optical and Electronic Information, Huazhong University of Science and Technology, Wuhan 430074, China.
E-mail addresses: sharshir@eng.kfs.edu.eg (S.W. Sharshir), jfzang@hust.edu.cn (J. Zang), nuo@hust.edu.cn (N. Yang).

https://doi.org/10.1016/j.desal.2020.114564
Received 23 February 2020; Received in revised form 25 May 2020; Accepted 1 June 2020

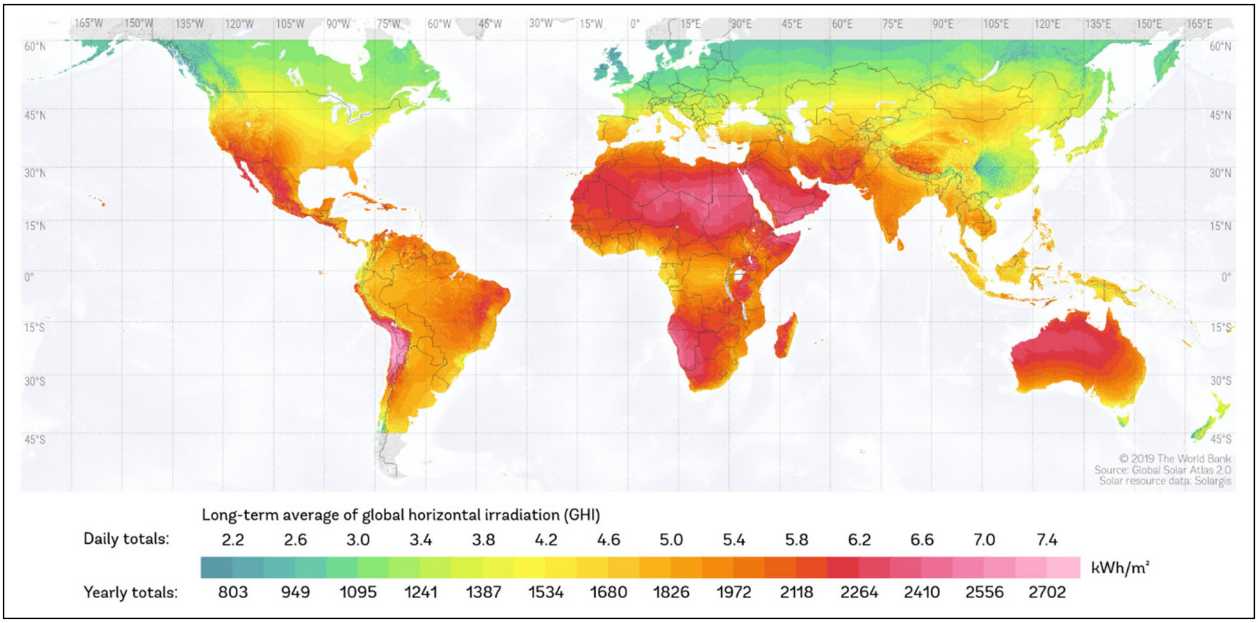

Fig. 1. Global horizontal solar irradiation (https://globalsolaratlas).

very widespread due to large productions and low energy consumptions compared with other technologies [21]. Over the past two decades, many RO desalination plants have been built with big capacity all over the world to compensate for water shortages [22]. It is well known that the process of traditional desalination consumes a large amount of energy and produces huge greenhouse gas emissions [21]. Also, a large number of marine organisms are killed during the transfer of water from and to traditional stations [23]. In addition, sufficient electrical power for large traditional desalination plants may not be available in some coastal areas and remote (i.e., no grid supply available) [24].

Recently, solar-driven water evaporation as a classical solar-thermal energy process has been widely examined due to its positive contribution in developing extensive applications such as sterilization [25], water treatment [26], wastewater remediation [27], desalination [28], and steam generation [29,30]. To improve the performance of vapor generation and desalination using SE, many factors have been taken into consideration, such as high photothermal conversion efficiency, a large specific surface area subjected to evaporation, hydrophilicity for fluid transport [31].

Solar stills, as one of the solar desalination technologies, have been well studied in terms of their productivity, efficiency, and economics [32]. Furthermore, researchers are still working to overcome the bottleneck of traditional solar still by optimizing the solar evaporation process based nanofluid materials [33–35]. Unfortunately, they still suffer from the low production rate and efficiency owing to large losses and a huge amount of energy needed for massive water heating and solar steam-generating. To overcome the previous defects of the traditional desalination processes, new notions of water-air interface solar heating have been recently developed depending on plasmonic nanoparticles [36–38], conjugated polymers [39], carbon-based materials [40–42], heat localization and thin film [43,44], bio-inspired nanostructures [45], mushrooms [46], aerogels [47–49] and hydrogels. All these materials are added to the evaporation surface to concentrate the heat on the water surface instead of heating the bulk water, improving the photothermal energy conversion, reducing heat loss, and augmenting the overall performance [50,51]. As a result, they can be utilized for improving traditional solar evaporation and desalination [39,52].

Furthermore, wastewater remediation based solar steam generation has also been gained much attention in the last few years and inspired researcher interests for contaminants removal and human health protection, accompanied by high effluent quality and cost reduction benefits. Due to the lower thermal conversion of solar light and the presence of organic contaminants, suspended solids and toxic metals in wastewater, fabrication of new material with high absorption of solar radiation, bacterial inactivation, and contaminant degradation are inevitably required [53,54]. Various types of photothermal and photocatalysis have been examined toward sunlight harvesting capability and wastewater treatment, in which semiconductor and carbon-based materials such as titanium dioxide (TiO_2), graphite, graphene, chitosan, carbon nanotube, molybdenum sulfide (MoS_2), cadmium sulfide and zinc oxide (ZnO) have brought great attention for its superior light absorption and photocatalytic activation [53,55–57].

Hydrogel is polymeric networks (porous matrixes) that consist of a large number of water molecules established by the cross-linking of polymers hydrophilic [58]. Hydrogels have been employed in various technologies and products such as inclusive artificial tissues [59], hygiene products [60], contact lenses [61], drug delivery [62], and agricultural fertilizers [63]. Moreover, hydrogels are features with large interior surface area, stabilized in the inseparable aqueous solutions, well reused and durable [64,65]. Many attempts have been conducted to investigate the structure and photothermal conversion efficiency solar steam generation using hydrogel material. Nanomaterials embedded within a hydrogel are energetically favored to improve the general properties that make it suitable for quick steam generation compared to the other materials [66–68]. Hydrogels have been involved in saltwater desalination as membrane-like barriers allowing limited salt ions passage and generating pure water by applying external pressure [69]. Some additives such as graphene oxide, gold, and silver nanoparticles or black Titania have been added to hydrogel-forming effective composites in water purification systems [70,71]. Interfacial solar steam generation-based hydrogel material fabrication is a novel way for scalable and real field applications for water purification and wastewater treatment [72–74]. More recently, composite hydrogel-based material demonstrated higher adsorption and removal efficiency compared with monolayer hydrogel material, which attributed to the uniqueness of the interior 3-D network structure [55,73–75].

In this paper, a comprehensive introduction and review of the works published using hydrogel materials in solar steam generation, water desalination, wastewater remediation, and industrial sewage are presented. Also, the various preparation and syncretization methods of the

hydrogels have been discussed. Further, a detailed comparison between hydrogel-based systems and other conventional ones is presented. Finally, the future-prospects of hydrogel materials and applications are discussed.

2. Hydrogel materials applied for water evaporation

Since 2017, hydrogel-based materials have considered as one of the most important materials used in the process of water evaporation and desalination, which proved a high-water evaporation rate and efficiency compared to the other materials, which ascribed to the heat localization symbiosis on the air-water interface. So far, literature has presented and proposed various hydrogel structures that were utilized at water evaporation and desalination applications. Applying hydrogel materials for water evaporation using solar energy requires adding of photothermal conversion material. Notably, it was found that air-water interface temperatures were triggered by incorporating photothermal absorbers on the hydrogel materials, which can increase the solar absorption and directly convert heat localization to the small amount of water surface. Therefore, hydrogel-based materials can be classified based on photothermal absorbers to three subsections, which involved nano-based photothermal conversion material, polypyrrole as photothermal conversion material, and other photothermal conversion materials.

2.1. Hydrogel materials with nano-based photothermal conversion absorbers

Due to the nanostructure of nano-based photothermal absorbers, the internal surface area is triggered, accompanied by higher utilization of solar radiation and increasing the air-water interface temperatures. Consequently, the solar radiation turns into thermal energy, which can be transferred to the small amount of water inside hydrogel material, concomitantly with higher evaporation rates, and enhance photothermal conversion efficiency.

Sun et al. [76] introduced a copper sulfide-microporous polyacrylamide (CuS-m-PAM) as a novel inorganic-organic light-absorbing hydrogel material, which was used to improve solar steam generation. After polymerization for acrylamide to obtain PAM, the salt leaching technique was performed to obtain m-PAM. CuS-m-PAM was prepared by placing m-PAM in $CuCl_2$ solution. The proposed material showed some advantages such as augmentation solar photothermal conversion of CuS nanoparticles, bond formation between CuS nanoparticles, and NH_2 groups in m-PAM, which provided stabilization for CuS nanoparticles, steam exhaust, and water replenishment was improved. The possible reason may be attributed to the microporous structure of m-PAM, which can reduce the heat losses in the transfer process due to the heat localization phenomena. Fig. 2(a) illustrates a scheme of steam generation device which used CuS-m-PAM as light-absorbing material and polyethylene foam wrapped in cotton cloth as thermal insulation and water supply module. CuS-m-PAM was prepared by $CuCl_2$ solution of 0.05 mol L^{-1} (CuS-m-PAM-0.05) and showed that it could reach a rate of evaporation equals 1.46 kg m^{-2} h^{-1} with a solar photothermal conversion efficiency of 92% under 1 sun illumination (1000 Wm^{-2}) as revealed in Fig. 2(b). Moreover, after 50 test cycles, the solar photothermal conversion efficiency was held on 87.5%, and excellent reusability highlighted.

Zhao et al. [77] studied a new composite hydrogel material prepared by graphene oxide (GO), silica aerogels (SA), acrylamide (AM), and polyvinyl alcohol (PVA). GO nanosheets provided hydrogel material by prominent photothermal conversion efficiency. SA has low density and ability of self-cleaning, so it provided the hydrogel material by floatability and made it suitable and durable for real applications. As a result of the low density of SA, which approaches the air density, it moved to the top of the hydrogel material forming a hydrophobic surface while the bottom layer was hydrophilic surface. So, the obtained material worked by water transportation, and the evaporation mechanism look like planets. The scanning electron microscopy for the top surface of GO/SA PAM-PVC hydrogel is shown in Fig. 3. By applying this newly merged hydrogel for vapor generation, the results showed that evaporation mass of seawater was triggered 6 times more than that obtained by the conventional process at a solar concentration of 2 sun radiance for 30 min.

On the other side, a novel double-layer hydrogel device by an easy and green process is fabricated by Sun et al. [78]. The top or light-harvesting layer consisted of silver nanoparticles (Ag NPs) and poly (sodium-p-styrenesulfonate) (PSS) with agarose gel (AG) skeleton, as shown in Fig. 4(a). PSS was used to prevent the aggregation and growth of Ag NPs. Because of Ag NPs, this layer worked for collecting and transferring light to heat efficiently. The bottom or water-collecting layer material was AG, which was the same one of the top layers to form a mesh network continuously between the two layers. Ag-PSS-AG/AG device was applied for steam production by modeled sewage and muddy water to study its capability of separation. Fig. 4(b) and (c) illustrates the device evaporation performance under model sewage and muddy water, respectively. Ag-PSS-AG/AG device showed a rate of steam production of 2.1 kg m^{-2} h^{-1} with a photothermal conversion efficiency of 92.8% at 1 sun radiance.

A hybrid anti-fouling hydrogel material which consisted of PVA as a hydrophilic base material and reduced graphene oxide (rGO) as a solar absorber is proposed by Zhou et al. [79]. In the hydrogel network, water evaporation became easy because PVA reduced enthalpy of water evaporation. Internal capillary channels in rGO made water transport in hydrogel easier, so this material was considered as a hydrogel with capillarity facilitated water transport (CTH). Fig. 5(a) shows a schematic of the proposed material and its solar vapor generation, and Fig. 5(b) illustrates the concentrations of ions in the real sample of seawater before and after the desalination process, while Fig. 5(c) elaborates on the concentrations of the ion and accumulation in CTHs during 96 h operation. Finally, the experimental results of using this material in solar vapor generation showed nearly ~2.5 kg m^{-2} h^{-1} at 96 h, as given in Fig. 5(d), with a photothermal conversion efficiency of ~95% at 1 sum radiance can be achieved.

A biomimetic water transportation and evaporation system that was inspired by conifer tracheid construction are introduced by Xu et al. [80]. The system contained a bottom layer of three-dimensional polyacrylamide (PAM) based aerogel with radial and concentric structure, which fabricated by using the low-temperature cross-linking method, and the upper layer of multi-wall carbon nanotubes for solar radiation harvesting. Radially aligned microchannels, porous network, wavy internal surface, and molecular meshes of the proposed material enabled it to good capillary rise performance and efficient antigravity water transportation. An experimental study was carried out to identify water evaporation rate and efficiency under 1 sun illumination for evaporating water alone, water with a single layer of the radial structure of PAM, and water with proposed material, which consisted of two layers. The results revealed that the proposed system exhibited higher performance with an evaporation rate of 2 kg m^{-2} h^{-1} and photothermal conversion efficiency of 85.7% under 1 sun illumination. To prove the stability and durability of the proposed material, it was tested for 50 cycles, in which the evaporation rate was ranged between 1.8 and 2 kg m^{-2} h^{-1}. Moreover, it was tested under real outdoor conditions with peak solar radiation of 0.7 sun illumination; consequently, the results showed that the evaporation rate is more than 1.5 kg m^{-2} h^{-1}. Furthermore, the proposed material maintained its transport and evaporation rates when it has experimented with seawater for 7 days. Yin et al. [81] fabricated macroporous double-network hydrogel of poly (ethylene glycol) diacrylate (PEGDA) and polyaniline (PANi), denoted as p-PEGDA-PANi. The experimental setup was carried out to investigate employing p-PEGDA-PANi hydrogel as light-absorbing (top layer) while cellulose wrapped expanded polyethylene foam as a water supply module (bottom layer) and thermal insulation in one solar steam

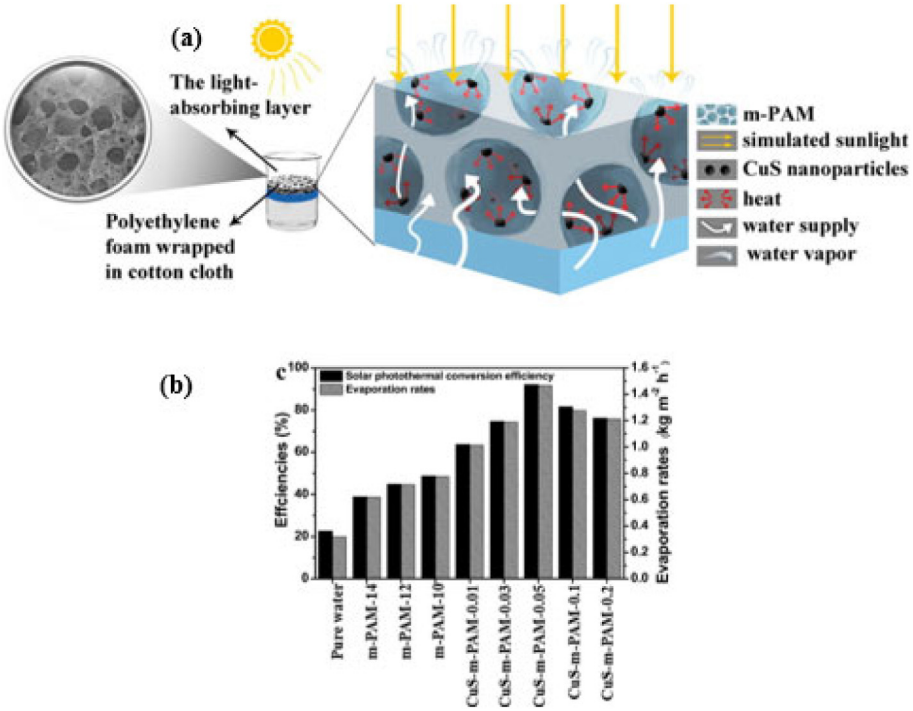

Fig. 2. (a) Schematic illustration of CuS-m-PAM hydrogel material, (b) rate of water evaporation, and conversion efficiency [76].
Copyright 2020 Elsevier.

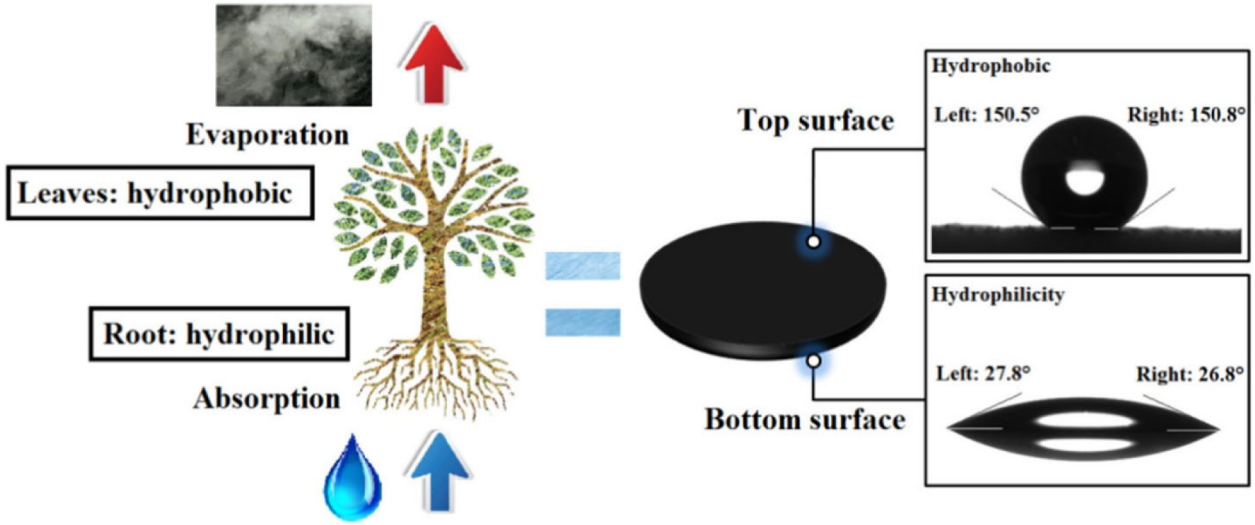

Fig. 3. A schematic illustration of the correlation between the seawater desalination and plant system, and the contact angles of water on the bottom and top surface [77].
Copyright 2020 Elsevier.

generation device. The proposed device exhibited a water rate of evaporation equals 1.4 kg m^{-2} h^{-1} under 1 sun illumination and with a maximum photothermal conversion efficiency of 91.5%. The proposed material is durable and stable; even it can maintain its energy conversion efficiency at 86.8% ± 3.9% after 50 cycles under 1 sun illumination. Furthermore, Guo et al. [82] introduced a light-absorbing sponge-like hydrogel that was produced by in situ gelations of PVA and uniformly distributed nanoparticles of titanium sesquioxide (Ti_2O_3), these nanoparticles have larger photothermal efficiency, so they were added for efficient solar radiation harvesting. Interaction between water, polymer, and nanoparticles led to synergistic energy nanoconfinement and low energy requirement for evaporation. Moreover, 3-D interconnected porous structure in the proposed hydrogel led to the rapid replacement of produced vapor by new water. Applying the proposed hydrogel on water evaporation revealed an ultrafast rate of evaporation equals ~3.6 kg m^{-2} h^{-1} with a photothermal conversion efficiency of ~90% under 1 sun illumination. It was observed that the proposed hydrogel was durable and stable enough to be used in solar water desalination with a large scale to cater to the human ever-increasing need for freshwater. Seawater samples were applied to evaporation with the aid of the proposed material and concentration of the following four ions before and after the desalination process; Na^+, Mg^{2+}, K^+ and Ca^{2+}.

The ultrasonic deposition-squeeze-ultrasonic removal process is applied for coating three different types of commercial sponges (PVA, polyurethane, and melamine) with carbon black nanoparticles [83]. In

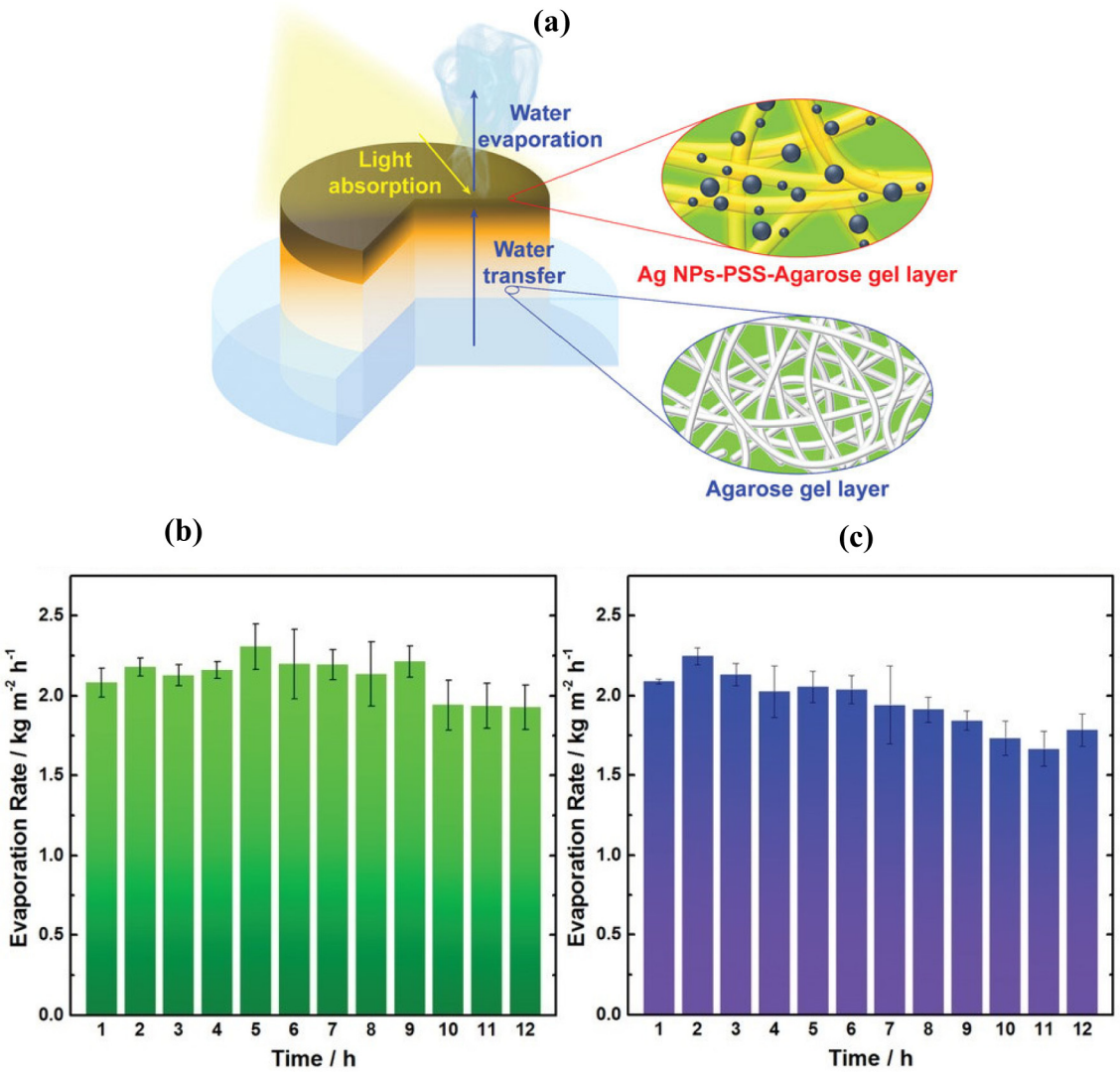

Fig. 4. Ag-PSS-AG/AG evaporation performance (a) schematic diagram of the double-layer based solar vapor generation under (b) model sewage and (c) model muddy water [78].
Copyright 2020 Wiley.

this work, carbon black nanoparticles attached to PVA sponge firmly while they were lost from other sponges' surfaces. The presence of carbon black nanoparticles and their high photothermal conversion efficiency led to high optical absorbance of solar radiation for coated PVA sponges, up to 96.5%. 3-D nano ink-stained PVA sponges were fabricated with dimensions of 2 × 2 × 1 cm and applied in a mimetic tree system (similar to the system discussed by Liu et al. [84]). Because of their stability, high evaporation area, and high photothermal conversion efficiency, the proposed PVA sponges exhibited a rate of evaporation equals 1.69 and 2.15 kg m^{-2} h^{-1} under 1 sun illumination for applying embossment configuration of single-layer and three-layer of them in the mimetic tree system, respectively. The coated PVA sponges showed their effectiveness under sewage water which contains many oil droplets by giving desalinated water with no oil content. Also, PVA sponges were tested under water with 5 and 0.5 g L^{-1} Cu^{2+} metal ions and methylene blue solution, respectively. Analysis of the resulting water showed that it doesn't contain any methylene blue molecules but contains 0.059 mg L^{-1} of copper ions which meets acceptable levels of the Chinese government drinking water standard. PVA sponges coated with carbon black nanoparticles are durable and stable as their evaporation rate fluctuated with only 5% over 20 test cycles.

2.2. Polypyrrole as photothermal conversion material in hydrogel materials

Polypyrrole is a dark black, light-absorbing, and an organic polymer. It can absorb the full spectrum of solar radiation and convert it into thermal energy. So, integrating hydrogel with these materials can enhance the photothermal conversion process, and improve the performance of water evaporation based solar energy utilization.

Zhou et al. [85] introduced a highly hydratable light-absorbing hydrogel that was used for solar vapor generation to reduce the required energy and accelerate solar water purification. It was fabricated by infiltrating polypyrrole (PPy), which worked as a light absorber into a matrix of PVA and chitosan. During the synthesis hydrogel, hydration has a positive potential, which enabled the hydrogel polymer chains to interact with nearby water molecules and make bonds with it such as hydrogen bonding, so bound water was formed. There was an opposite water molecule called free water, which was separated from polymer chains, and between two mentioned types of water molecules, there was intermediate water. After conducting experiments for applying this material for solar vapor evaporation, the results showed that intermediate water requires less evaporation energy compared with bulk water, which leads to a reduction in overall required energy for evaporation. Applying h-LAH on solar water evaporation showed that an

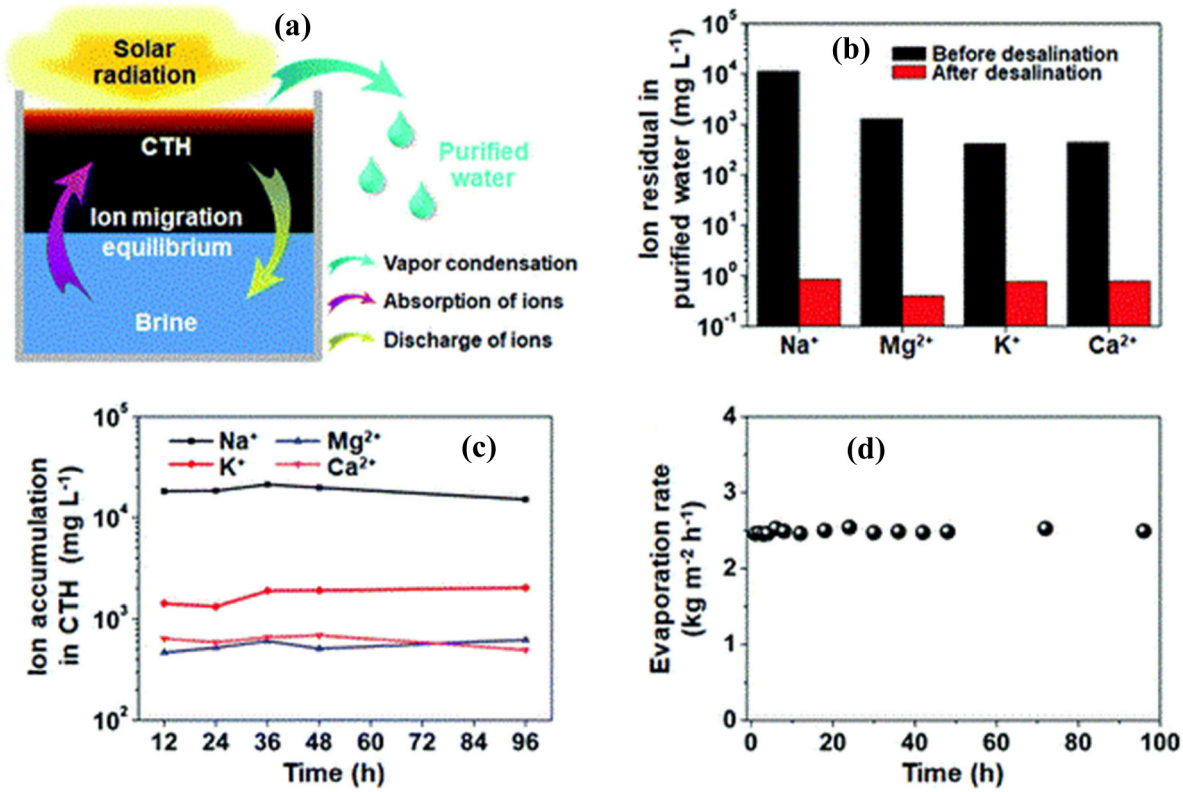

Fig. 5. (a) Schematic of hydrogel material based on PVA and rGO, (b) ions concentrations before and after desalination, (c) ions concentrations, and accumulated in CTHs during a time, and (d) evaporation rate [79].
Copyright 2020, Royal Society of Chemical.

evaporation rate of 3.6 kg m^{-2} h^{-1} under 1 sum illumination could be achieved with a photothermal conversion efficiency of ~92%. To ensure the reliability and effectiveness of the proposed material, it was tested under strong alkali and acid solutions, and the obtained distilled water pH value was ~7. Also, the material was examined with water containing four of the most known heavy metal ions; Pt^{2+}, Zn^{2+}, Cu^{2+}, and Ni^{2+}, then the resulting evaporation rate illustrated the stability of the proposed material. Furthermore, a large amount of freshwater production (18–23 Lm^{-2} per day) was reported by Zhao et al. [86] who presented a new hydrogel material and applied it to the solar water purification prototype. The proposed material was a hierarchically nanostructured gel which consisted of PVA and PPy because of their previously mentioned and required properties. The hierarchical porous structure of hierarchically nanostructured gel contained internal gaps, micron channels in the molecular meshes. This structure was responsible for providing water uniformly to the hydrogel network from bulk water. Applying this material on solar vapor generation led to a vapor generation rate of 3.2 kg m^{-2} h^{-1} with a photothermal conversion efficiency of ~94% at 1 sun radiance. Where the hierarchically nanostructured gel (HNG) and HNG1, HNG2, HNG3, and HNG4 represented gels with water/PVA weight ratios of 1:0.2, 1:0.15, 1:0.1 and 1:0.075, respectively. As an indication of the reliability and durability of the proposed material, the water evaporation rate was stable when the material was exposed to seawater and 1 sum illumination for 28 days.

Ni et al. [87] adopted in situ oxypolymerization of pyrrole to produce PPy cellulose paper (PPyP), which was a strong and cost-effective material. PPyP can be micro-/macroscopically controlled as its tunable microstructure enables us to control its water evaporation via balancing the factors of water transportation and light absorption, as shown in Fig. 6(a) and (b). Moreover, it can be folded into 3-D shape and switched back to its 2-D shape in a cycled manner efficiently, quickly, easily, and with good remolding capability. Two geometries of PPyP were prepared: 2-D model and 3-D model inspired by kid's game named cootie catcher. The models were fixed on polystyrene foam with good thermal isolation property and applied for water evaporation under various and extreme conditions. The results of indoor experiments under 30 °C ambient temperature and 50% humidity showed that the 3-D structure could reach a rate of evaporation equals 2.99 kg m^{-2} h^{-1} under 1 sun. Outdoor experiments were carried out. To examine the durability and stability of PPyP, it was immersed in HCl solution and seawater for a month, and no breakage was remarked on the material. Fig. 6 illustrates the solar vapor generation and photothermal, (a) reflection (b) absorption from 400 nm to 2400 nm wavelength, (c) different vapor temperature of water and PPyP on the air/water interface at 1 sun. (d) Change in temperature of water and P-1, (e) mass change of water, and various PPyP under one sun and dark condition with time. (f) Comparison of the mass change and evaporation efficiency at one sun, (g) profiles of temperature. (h) Mass change at different solar concentrations. (i) Thermal efficiency and evaporation rate at different solar concentrations.

Additionally, Wang et al. [88] developed a novel PPy-Fe_x-O_y-CTS gel membrane, which was fabricated by synthesizing PPy in chitosan (CTS) sol in situ. PPy and CTS were selected because of their brilliant photothermal and swelling features, respectively. Applying the proposed gel in water evaporation showed that the rate of evaporation equals 1.93 kg m^{-2} h^{-1} is achievable under 1 sun radiance, 30% humidity, and 25 °C room temperature. Furthermore, the average amount of water desalination was about 1.24 kg m^{-2} h^{-1} and freshwater output per day of 13.68 kg m^{-2} was observed under sunlight. On the other hand, a bi-layer polymer that consisted of pre-pressed melamine foam (MF) as a lower layer and PPy as the upper layer was investigated by Li et al. [89]. The PPy layer can absorb sunlight and evaporate water while MF can transport water and confine the energy to the evaporative

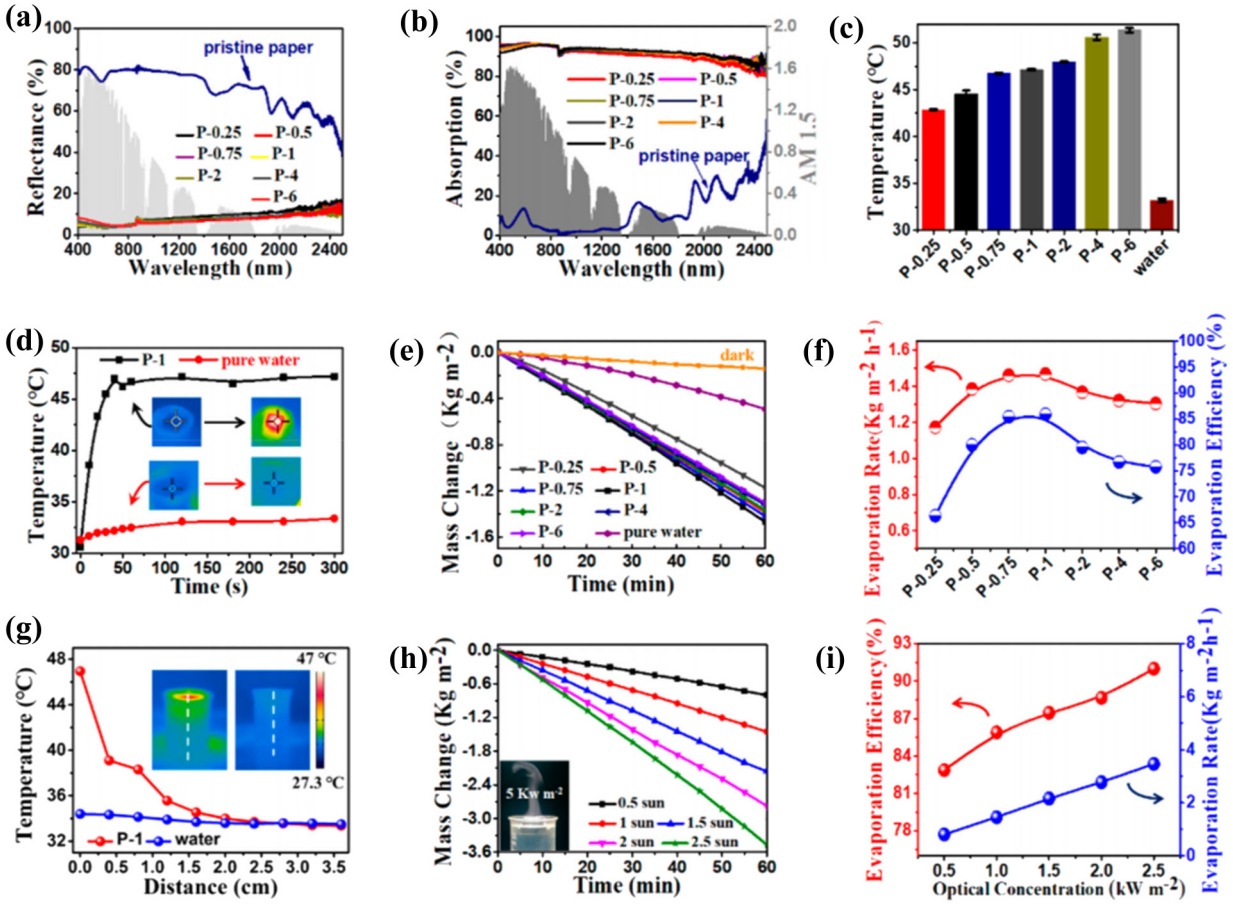

Fig. 6. Performance of prepared PPyP according to solar vapor generation, photothermal, and optical [87].
Copyright 2020, American Chemical Society.

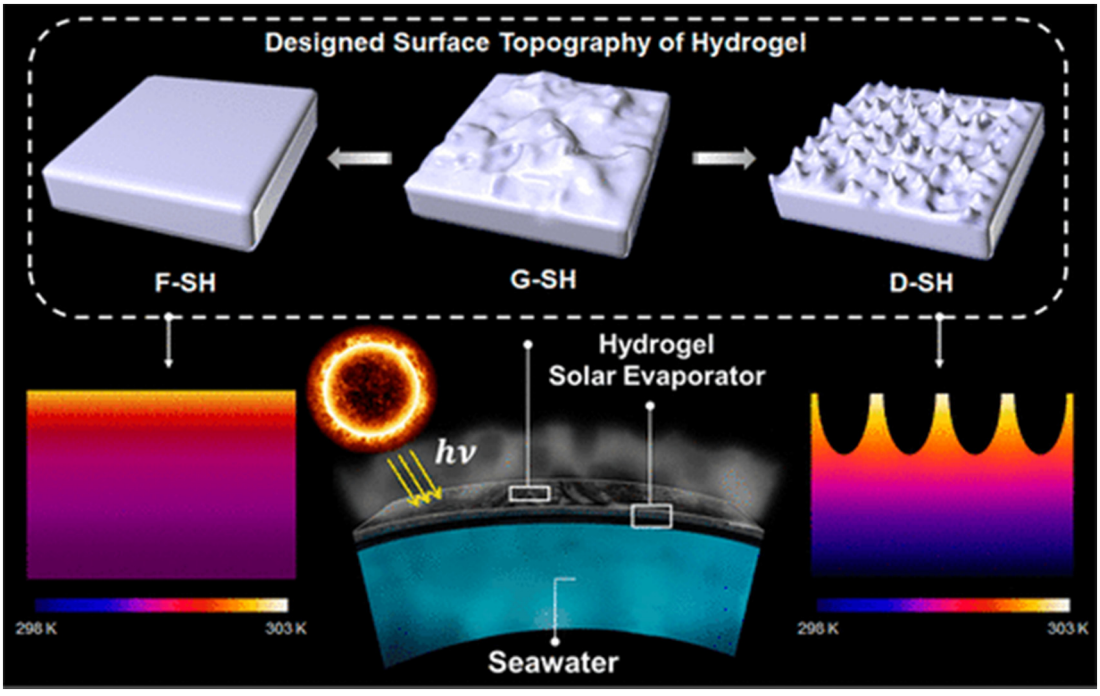

Fig. 7. Schematic of PVA hydrogel with a sharply dimpled surface in nanoscale [93].
Copyright 2020, American Chemical Society.

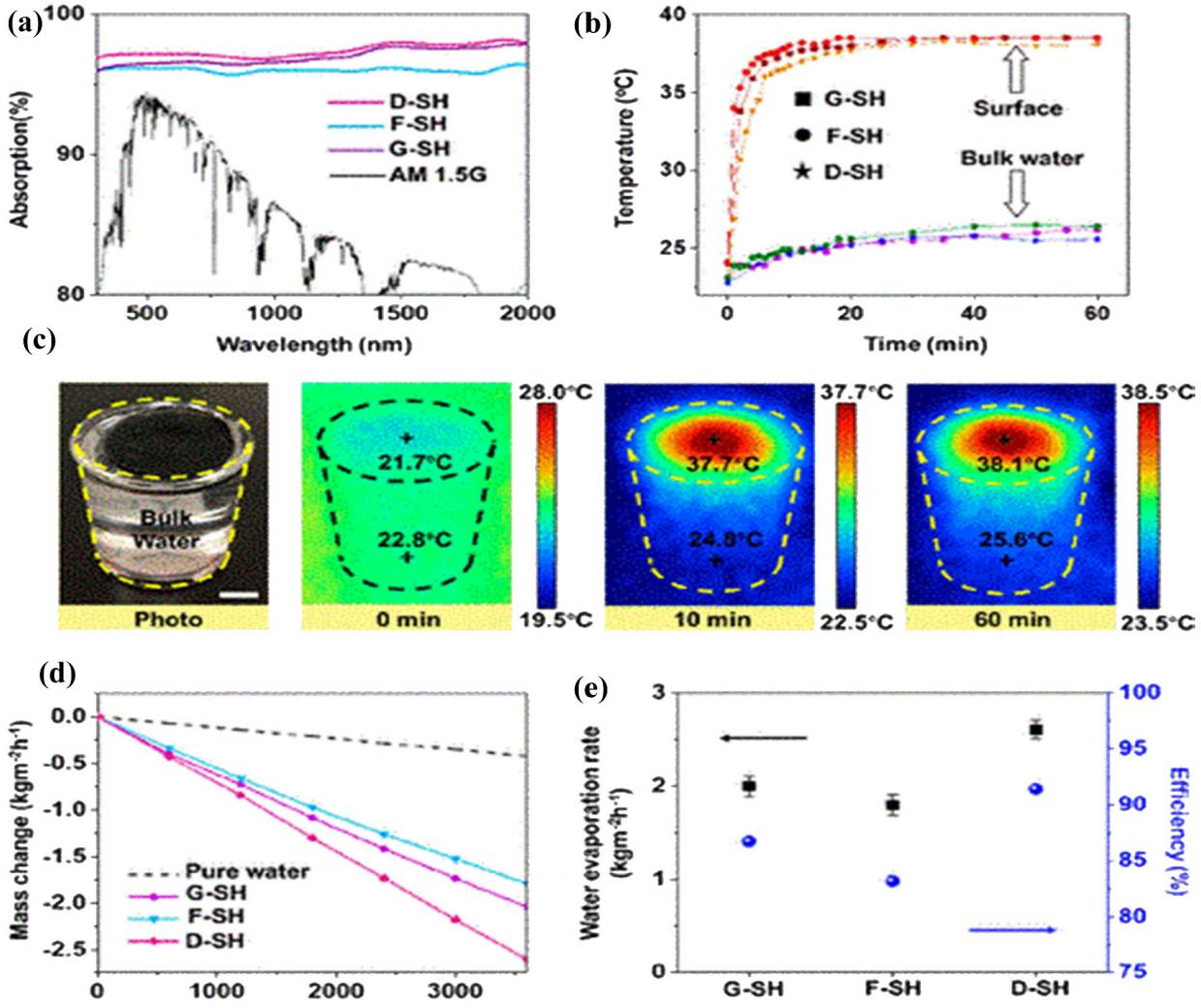

Fig. 8. Solar evaporation based on SHs. (a) Absorption. (b) The measured temperatures at bulk water and evaporation surface. (c) Infrared images illustrate the temperature distribution at different times at 0, 10, and 60 min. (d) Mass change. (e) The energy efficiency and evaporation rate. [93]. Copyright 2020, American Chemical Society.

surface via insulation. The material showed excellent anti-fouling property, durability, and good reusability so that it maintained its performance after 30 days with daily one-hour testing. Two possibilities of water desalination systems that use the proposed bi-layer polymer were investigated for on land and on water solar water desalination systems. Applying the proposed material in water evaporation revealed that a rate of evaporation equals 1.574 kg m^{-2} h^{-1} under 1 sun illumination with a photothermal conversion efficiency of 90.4% was achievable. Furthermore, the proposed material has experimented under natural sunlight and real outdoor conditions, consequently it showed its practical effectiveness. For assessment of desalination effect, ions concentration of Ca^{2+}, K^{+}, $Mg^{2+,}$ and Na^{+} were evaluated before and after the desalination process, the outcomes revealed that ions concentration is reduced by 99.93%.

2.3. Other photothermal conversion materials applied for hydrogel materials

In addition to nanomaterials and polypyrrole, there are other materials were added to hydrogel materials to perform a photothermal conversion process efficiently. Tan et al. [90] added conducted polymer hollow spheres (CPHSs) in their hybrid hydrogel material for enhancing solar radiation absorption and photothermal conversion capability. The proposed hydrogel material consisted of PVA and it also contained SA for density reduction and heat localization. Because of freezing the proposed hybrid hydrogel after mixing its ingredients, it has macro-sized channels for rapid water supply. Experimental results of using this material for solar vapor generation showed an evaporation rate of 1.83 kg m^{-2} h^{-1} with a photothermal conversion efficiency of 82.2% at 1 sum illumination. Furthermore, the evaporation test was repeated for 30 cycles, and the results did not show any decline in neither evaporation rate nor photothermal conversion efficiency. Additionally, Carbon-based composites of protonated g-C_3N_4 and GO were utilized as photothermal conversion material by Su et al. [91], who applied a simple hydrothermal co-assembly method on melamine and GO raw materials to prepare the protonated g-C_3N_4/graphene oxide hybrid hydrogel. Applying the proposed hydrogel material on water evaporation showed an average evaporation rate of 4.11 kg m^{-2} h^{-1} under 3 sun illuminations and photothermal conversion efficiency of 94.5%. The experiments were carried out for water with 3.5 and 5 wt% NaCl; consequently, the salinity by mg per liter was changed from 36,000 to 12.09 and from 100,000 to 7.17, respectively. It was concluded that the proposed hydrogel material is a self-floating hydrogel and can convert solar energy into thermal energy, as well as pump underneath the water to produce steam continuously. The proposed material is stable and durable, as proved by maintaining the material its performance after 5 test cycles. On the other side, Singh et al. [92] fabricated a porous chitosan/carboxymethyl cellulose hydrogel with embedded carbon dots

Table 1
Different hydrogel materials proposed for solar water evaporation and related perfomance.

References	Proposed materials	Photothermal conversion material	Hydrophilicity & hydrophobicity	Channels and pore size	Solar intensity/ kW	Mass change, kg m^{-2} h^{-1}	Thermal efficiency, %	Durability and duration of the test
Sun et al. [76]	Copper sulfide-microporous polyacrylamide (CuS-m-PAM) + polyethylene foam wrapped in cotton cloth as a lower layer	CuS nanoparticles	The two layers are hydrophilic	265.5 μm	1	1.4	92	Maintained its performance after 50 test cycles
Zhao et al. [77]	Graphene oxide/silica aerogel polyacrylamide-polyvinyl alcohol (GO/SA PAM-PVC)	GO nanosheets	Upper layer (hydrophobic), and bottom layer (hydrophilic)	Upper layer (1–4 μm), and bottom layer (5–12 μm)	2	Higher than conventional by 6 times	–	Its ability to self-cleaning made it suitable for reprocessing and reutilizing for real applications.
Sun et al. [78]	Upper layer of silver nanoparticles and poly (sodium-p-styrenesulfonate) with agarose gel + agarose gel as bottom layer (Ag-PSS-AG/AG)	Ag nanoparticles	Hydrophilic	–	1	2.1	92.8	–
Zhou et al. [79]	Polyvinyl alcohol + reduced graphene oxide (PVA + rGO)	rGO	Hydrophilic	Capillary channels with a diameter of 10 μm + pore size of several microns	1	2.5	95	Anti-fouling properties and ability of water desalination for a long time.
Xu et al. [80]	Poly acrylamide (PAM) + multi-walled carbon nanotubes	Multi-walled carbon nanotubes	Hydrophilic	Pore size of 2 μm in the center and increases with distance from center to reach 5–10 μm	1	2	85.7	Maintained its performance for 50 test cycles under
Yin et al. [81]	Hydrogel of poly (ethylene glycol) diacrylate and polyaniline (p-PEGDA-PANi) + cellulose wrapped expanded polyethylene foam as a bottom layer	PANi nanowires	hydrophilic	Pore diameter of 270–325 μm	1	1.4	91.5	Maintained its photothermal conversion efficiency at 86.8% ± 3.9% even after 50 test cycles
Guo et al. [82]	Polyvinyl alcohol + titanium sesquioxide nanoparticles (PVA + Ti_2O_3 nanoparticles)	Ti_2O_3 nanoparticles	Hydrophilic	–	1	3.6	90	–
Deng et al. [83]	Three layer of polyvinyl alcohol (PVA) sponges + carbon black nanoparticles	Carbon black nanoparticles	Hydrophilic	Pore size of 52 μm	1	2.15	–	Maintained its evaporation rate after 20 test cycles
Zhou et al. [85]	Matrix of polyvinyl alcohol (PVA) and chitosan + polypyrrole (PPy)	PPy	Hydrophilic	Pore size of several microns	1	3.6	92	Maintained its performance under strong alkali and acid solutions, and water containing heavy metal ions.
Zhao et al. [86]	Polyvinyl alcohol + polypyrrole (PVA + PPy)	PPy	Hydrophilic	Pore size of 150 μm	1	3.2	94	Maintained its performance when it was exposed to seawater and 1 sum illumination for 28 days
Ni et al. [87]	Polypyrrole cellulose paper (PPyP)	PPy	Hydrophilic	–	1	3	–	No breakage was observed on the material after immersion it into HCl solution and seawater for a month
Wang et al. [88]	Polypyrrole-Fe_x-O_y-chitosan (PPy-Fe_x-O_y-CTS)	PPy	Hydrophilic	–	1	1.93	–	–
Li et al. [89]	Melamine foam as a bottom layer + polypyrrole (PPy) as an upper layer	PPy	Bottom layer (hydrophobic) and upper layer (hydrophilic)	Bottom layer 100–200 μm and upper layer 8.4–50 μm	1	1.57	90.4	Maintained its performance after 30 days with daily 1 h of testing
Tan et al. [90]	Polyvinyl alcohol + silica aerogel + conducting polymer hollow spheres (PVA + SA + CPHSs)	CPHSs	Bottom layer (hydrophilic) and upper layer (hydrophobic)	Channel size ranges between several to 100 μm and pore size is 10 μm	1	1.83	82.2	Maintained its performance after 30 test cycles
Su et al. [91]	Protonated g-C_3N_4/graphene oxide (GO)	Carbon-based composites of protonated g-C_3N_4 and GO	Hydrophobic	Pore size of 12 μm	3	4.11	94.5	Maintained its performance after 5 test cycles under 3 sun illumination
Singh et al. [92]	Porous chitosan/carboxymethyl cellulose hydrogel with embedded carbon dots	Carbon dots	Hydrophilic	–	1	1.4	89	Maintained its performance after 50 test cycles

(*continued on next page*)

Table 1 (*continued*)

References	Proposed materials	Photothermal conversion material	Hydrophilicity & hydrophobicity	Channels and pore size	Solar intensity/ kW	Mass change, kg m^{-2} h^{-1}	Thermal efficiency, %	Durability and duration of the test
Guo et al. [93]	Polyvinyl alcohol (PVA) + activated carbon	Activated carbon	Hydrophilic	–	1	2.6	91	–

to enhance the photothermal properties of this composite material. The proposed material was made-up of simple and easy one-step, covalent conjugation of composite components by using cross-linker such as epichlorohydrin. This material revealed a good performance for water desalination as it reached a rate of evaporation equals 1.4 kg m^{-2} h^{-1} with a photothermal conversion efficiency of 89% considering 1 sun illumination. The results showed that the photothermal conversion efficiency remains above 85% even after 50 cycles of using the material which proved its durability, reusability, and stability. Moreover, the proposed material has bio-compatibility, recyclability, and environmentally friendly properties that makes it a suitable material for cleaner production of water with a high evaporation rate and good efficiency. Also, the material showed high removal efficiency of heavy metal ions from water, such as Cu^{2+}, Ni^{2+}, Ag^{+}, and Cd^{2+}. Guo et al. [93] adopted an in situ template-assisted gelation method to fabricate PVA hydrogel and made its surface sharply dimpled in nanoscale to increase heat flux at the evaporation front. Activated carbon paper was added to hydrogel as a bottom layer to absorb solar flux. Fig. 7 schematically illustrates the configuration of the proposed hydrogel and its application for solar water evaporation. The proposed hydrogel covered saline water, and solar energy drove the desalination process. The outcomes revealed that the discussed solar water evaporator could achieve a rate of evaporation equals ~2.6 kg m^{-2} h^{-1} with a photothermal conversion efficiency of ~91% at 1 sun radiance, as shown in Fig. 8(d) and (e). This hydrogel indicated effective desalination as it was applied for seawater with 3.5 wt% salinity. The results showed that Ca^{2+}, K^{+}, $Mg^{2+,}$ and Na^{+} ions concentrations in the resulting water were reduced by 2 or 3 times compared to reference water. The electric resistance of the collected steam generation was evaluated, which indicated that the resistance was increased by ~401%.

Different hydrogel materials proposed for solar water evaporation and related perfomance are summarized in Table 1. From this table, can compare and analyze the results of materials testing. It is noteworthy that PVA and chitosan achieved the highest water evaporation rate, due to their ability to sustainable transportation of water through the microporous structure of hydrogels and compensate lost water in evaporation, which permits heat localization to carry out on the air-water interface. Furthermore, nanomaterials are very suitable as photothermal conversion materials as they showed a distinct conversion efficiency, which reached 95%. Also, adding them to hydrogel materials during the synthesis process is very simple. PPy showed a great photothermal conversion efficiency, too. While CPHSs gave the lowest conversion efficiency.

According to the literature, there are many types of water that have been investigated. In addition, the water quality before and after the desalination process have evaluated via different indicators. Commonly, these indicators are pH value and salinity or total dissolved solids (TDS) that measure contained elements and ions (Na^{+}, Mg^{2+}, Ca^{2+}, K^{+}, Cu^{2+}, Ni^{2+}, Cd^{2+}, Ag^{+}, methylene blue, Zn^{2+} and Pb^{2+}). Table 2 summarizes all proposed types of water and their quality before and after desalination using hydrogel materials.

3. Hydrogel materials applied for water cleaning

Currently, clear water production is inevitably needed either for drinking purposes or agriculture reuse applications. In the preceding section, water evaporation and desalination by the aid of hydrogel materials were demonstrated and discussed. Herein, due to the energy crisis, we discuss the application of hydrogel materials in water cleaning and production processes application in order: water generation from the atmosphere, water cleaning and quality maintenance, and Forward osmosis water desalination with high permeable flux and fast water release.

Li et al. [94] fabricated a flexible hybrid atmospheric water generator material composed of deliquescent salt ($CaCl_2$), hydrogel material (PAM), and carbon nanotubes. The conceptual design for the

Table 2
Summary of water properties before and after desalination.

References	Water type	Properties of used water	Properties of produced water
Sun et al. [76]	3.4 wt% simulated seawater	10,000, 1000, 600 and 300 mg L^{-1} of Na^+, Mg^{2+}, Ca^{2+} and K^+, respectively	0.3, 0.1, 0.08 and 0.03 mg L^{-1} of Na^+, Mg^{2+}, Ca^{2+} and K^+, respectively
Sun et al. [78]	30 wt% SiO_2 water colloid	Electric resistance between constant distance electrodes is 0.196 MΩ	Electric resistance between constant distance electrodes is 0.747 MΩ
	Water-based carbon ink	Electric resistance between constant distance electrodes is 0.512 MΩ	Electric resistance between constant distance electrodes is 0.996 MΩ
	1:1 muddy water	–	Electric resistance between constant distance electrodes is 0.585 MΩ
Zhou et al. [79]	Seawater from Gulf of Mexico	10,000, 1000, 500 and 400 mg L^{-1} of Na^+, Mg^{2+}, Ca^{2+} and K^+, respectively	0.9, 0.4, 0.7 and 0.7 mg L^{-1} of Na^+, Mg^{2+}, Ca^{2+} and K^+, respectively
Xu et al. [80]	Seawater from East China sea	9000, 1000, 300 and 400 mg L^{-1} of Na^+, Mg^{2+}, Ca^{2+} and K^+, respectively	0.8, 0.09, 0.1 and 0.7 mg L^{-1} of Na^+, Mg^{2+}, Ca^{2+} and K^+, respectively
Guo et al. [82]	Seawater from Gulf of Mixeco	10,000, 1000, 400 and 400 mg L^{-1} of Na^+, Mg^{2+}, Ca^{2+} and K^+, respectively	3, 0.2, 0.8 and 0.2 mg L^{-1} of Na^+, Mg^{2+}, Ca^{2+} and K^+, respectively
Deng et al. [83]	Mixed pollutant	5000 and 500 mg L^{-1} of Cu^{2+} and methylene blue, respectively	0.059 and 0 mg L^{-1} of Cu^{2+} and methylene blue, respectively
Zhou et al. [85]	Seawater from Gulf of Mexico	10,000, 1000, 400 and 400 mg L^{-1} of Na^+, Mg^{2+}, Ca^{2+} and K^+, respectively	9, 7, 5 and 2 mg L^{-1} of Na^+, Mg^{2+}, Ca^{2+} and K^+, respectively
	Polluted water with heavy metal ions	40, 70, 100 and 200 mg L^{-1} of Ni^{2+}, Cu^{2+}, Zn^{2+} and Pb^{2+}, respectively	0.06, 0.4, 0.4 and 0.09 mg L^{-1} of Ni^{2+}, Cu^{2+}, Zn^{2+} and Pb^{2+}, respectively
Zhao et al. [86]	Artificial seawater with salinity of 0.8 wt %	–	Water salinity of 0.0003 wt%
	Artificial seawater with salinity of 3.5 wt %	–	Water salinity of 0.0002 wt%
	Artificial seawater with salinity of 10 wt %	–	Water salinity of 0.0005 wt%
	Seawater from Gulf of Mexico with	10,000, 1000, 400 and 400 mg L^{-1} of Na^+, Mg^{2+}, Ca^{2+} and K^+, respectively	2, 0.9, 0.2 and 0.6 mg L^{-1} of Na^+, Mg^{2+}, Ca^{2+} and K^+, respectively
Ni et al. [87]	Seawater	10,000, 400, 400 and 400 mg L^{-1} of Na^+, Mg^{2+}, Ca^{2+} and K^+, respectively	0.4, 0.8, 1 and 0.4 mg L^{-1} of Na^+, Mg^{2+}, Ca^{2+} and K^+, respectively
Wang et al. [88]	Domestic sewage	Total dissolved salts (TDS) of 249 mg L^{-1} and pH value of 7.86	Total dissolved salts (TDS) of 25 mg L^{-1} and pH value of 6.72
Li et al. [89]	Seawater from Yellow sea, China	10,000, 1000, 100 and 400 mg L^{-1} of Na^+, Mg^{2+}, Ca^{2+} and K^+, respectively	0.8, 0.1, 0.09 and 0.2 mg L^{-1} of Na^+, Mg^{2+}, Ca^{2+} and K^+, respectively
Su et al. [91]	Simulated seawater with 3.5 wt% salinity	36,000 mg L^{-1} salinity	12.09 mg L^{-1} salinity
	Simulated seawater with 10 wt% salinity	100,000 mg L^{-1} salinity	7.17 mg L^{-1} salinity
Singh et al. [92]	Saline water with a salinity of 10 wt%	Salinity of 10 wt%	Salinity less than 0.001 wt%
	Water with dissolved heavy metal ions	Contains ions of Cu^{2+}, Ni^{2+}, $Cd^{2+,}$ and Ag^+	All ions concentrations are less than 0.05% of their initial concentrations
Guo et al. [93]	Seawater from the Gulf of Mexico with salinity of 3.5 wt%	10,000, 1000, 400 and 400 mg L^{-1} of Na^+, Mg^{2+}, Ca^{2+} and K^+, respectively	40, 3, 8 and 10 mg L^{-1} of Na^+, Mg^{2+}, Ca^{2+} and K^+, respectively

proposed hydrogel as an atmospheric water generator is schematically illustrated in Fig. 9. Deliquescent salt was responsible for excellent water sorption capacity even in small relative humidity of the proposed material, while hydrogel maintained the solid form of it after large water quantity sorption. An outdoor experiment was conducted using 35 g of a dry hydrogel, and it provided 20 g of freshwater after 2.5 h. It was concluded that using this technology for providing fresh water for an adult minimum water consumption per day (i.e., 3 kg) costs only 3.2 $, so it is a cheap and affordable atmospheric water generator type. Always, a single step of free-radical UV-induced polymerization was adopted by Wang et al. [95] for acrylamide (AM) and acrylic acid anti-fouling materials to fabricate a support for titanium dioxide nanoparticles (TiO_2 NPs). The produced hydrogel exhibited antibacterial, photocatalytic, and good mechanical strength properties, so the possibility of applying it for water quality maintenance in pothos hydroponic plants was investigated. For hot summer conditions, water used for the hydroponic plant is exchanged with high frequency as the amount of dissolved oxygen in this water is reduced, and plant roots rot. Using the proposed hydrogel revealed a lower total organic carbon concentration in the plant water and efficient oxidation of TiO_2 NPs photocatalysis which reduced the environmental impact of soil-less system. This hydrogel is a good choice for hydroponic plants in arid regions as it lowers water exchange frequency.

Zeng et al. [96] applied free-radical UV-induced polymerization on sodium acrylate and N-isopropylacrylamide (NIPAAm) monomers with different mixing ratios to produce various samples of P(NIPAAM-co-sodium acrylate) and investigate their polyelectrolyte concentration. Samples with zero concentration of sodium acrylate were denoted by P-NIPAAm. A novel multilayer hydrogel was investigated to combine high osmotic pressure advantage provided by P (NIPAAM-co-sodium acrylate) and fast water release advantage provided by P-NIPAAm. This hydrogel was fabricated with single, double, and multilayers, and every layer was fabricated with various mixing concentration ratios between NIPAAm and sodium acrylate monomers. Various samples were applied for forward-osmosis desalination to enhance its performance. A three-layer hydrogel sample with gradually decreased sodium acrylate concentration (sodium acrylate to NIPAAm mixing ratios were 1:1, 0.5:1 and 0:1 for drawing, intermediate and releasing layers, respectively) showed its ability for releasing ~60% from the absorbed water in 60 min at its fully swollen state while another hydrogel sample of a single layer with sodium acrylate to NIPAAm mixing ratio of 1:1 released only ~35%from its absorbed water. The observed results showed that multilayer hydrogels could develop energy-efficient forward osmosis desalination.

4. Wastewater remediation and ions adsorption-based hydrogel materials

The recycling and treatment of wastewater with cost reduction benefits are inevitably needed for humankind's survival. Conventional

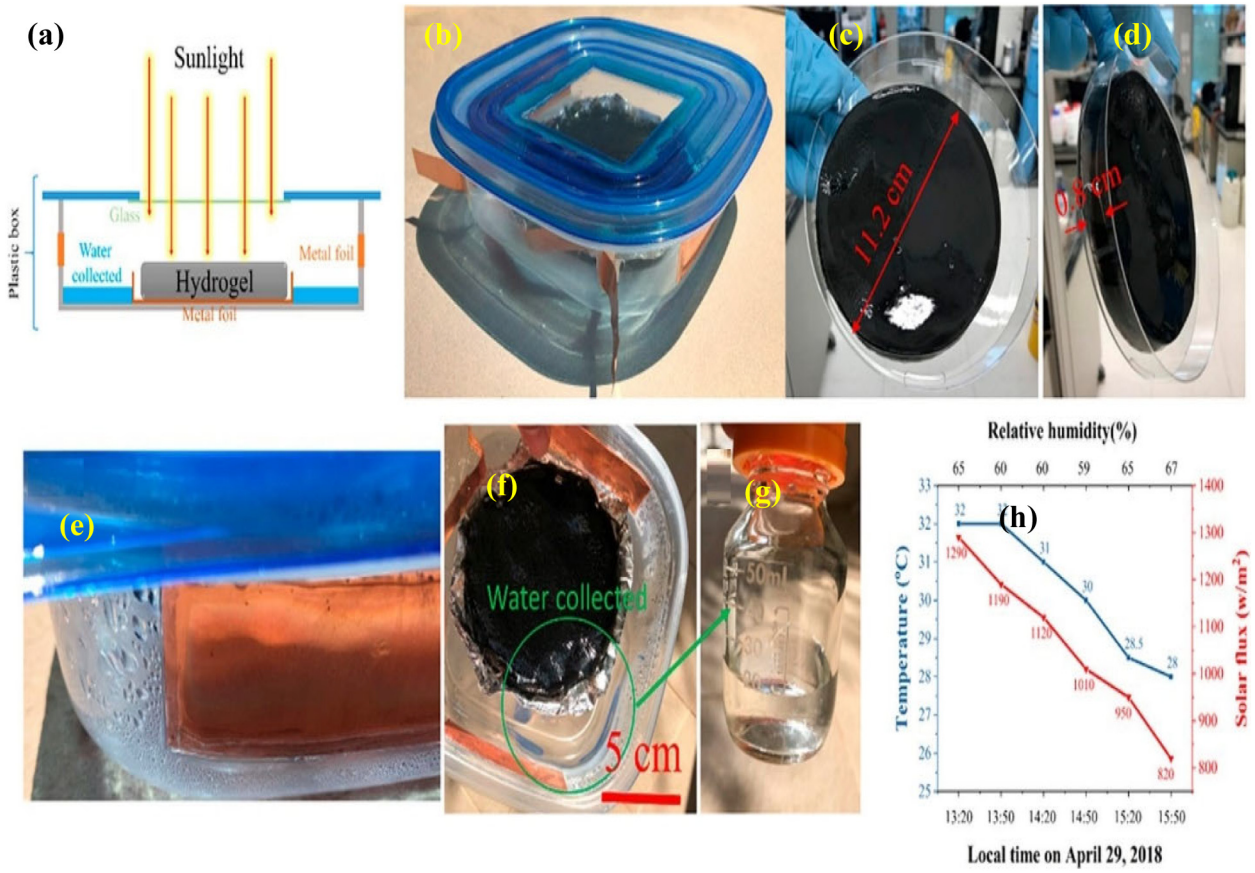

Fig. 9. (a) Schematic of applying hydrogel based on $CaCl_2$, PAM, and carbon nanotubes for atmospheric water generation, (b) collection water device prototype established on PAM–CNT–$CaCl_2$ hydrogel. (c, d) Illustration of the dimension of PAM–CNT–$CaCl_2$ hydrogel. (e) water condensation. (f) Photo of the hydrogel after water release. (g) Freshwater, and (h) meteorological conditions (air temperature and solar radiation) [94].
Copyright 2020, American Chemical Society.

water purification and wastewater treatments are energy consumer technologies besides they inefficiently effluent water quality (i.e., physical, chemical, and biological processes [54]). In this section, we demonstrate and discuss hydrogel materials applied even for adsorption or catalysis of impurities and ions from wastewater to get clean and potable water. Hydrogel materials proved their effectiveness in low-cost wastewater remediation, industrial sewage, and ions adsorption, so they are advantageous compared to other conventional water treatment methods.

Bisphenol A (BPA) is the material used for producing certain resins and plastics which are used in food containers and water bottles industry [97]. Due to the steadily increasing of BPA production, it is heavily released in water, so many researchers are interested in removing it from water [98,99]. Zhu et al. [55] fabricated a composite photocatalytic hydrogel-based cadmium sulfide for efficient degradation of (BPA) from polluted wastewater. The synergistic effect of heterogeneous photocatalyst P(HEA-co-HAM)-CdS and presence of CdS in the hydrogel led to high adsorption capacity and degradation rate. As resulted, as much as the degradation rate of 92% in 3 h and TOC removal of 47% was remarked. As shown in Fig. 10, the adsorption photo-oxidative optical properties and swelling ratio of the heterogeneous hydrogel are better than P(HEA-co-HAM) hydrogel. As, the presence of cadmium sulfide (CdS) promotes more solar energy due to the narrow bandgap of 2.4 eV.

On the other way, Panao et al. [100] fabricated a hybrid hydrogel by covalent gelation of alginate in the presence of vinylated-SiO_2. The proposed hydrogel showed high water absorption as it was observed that 1 g dry of this material could absorb 889.76 ± (12.65) g of water. Applying this hybrid hydrogel for methylene blue removing from the water was investigated, and results showed that increment in modified alginate and monomer amount and decrement in vinylated-SiO_2 amount leads to increment and reduction in methylene blue removal, respectively. In different circumstances, Lee et al. [101] introduced a simple one-step method to fabricate copper ferrocyanide-embedded hydrogel beads (CuFC-MHBs), which were able to remove cesium from water efficiently and can be separated magnetically. CuFC-MHBs were fabricated by a simple interaction between potassium ferrocylanide and copper at 5 wt% of PVA. X-ray diffraction, FTIR spectroscopy, SEM, and vibrating sample magnetometry were conducted to detect the content, structure, and magnetic properties of CuFC-MHBs. It was observed that the magnetic responsiveness and cesium adsorption ability of CuFC-MHBs could be controlled by regulating the ratio of feed weight of copper salt to PVA while using a fixed molar ratio of Cu to ferrocyanide (3:1). The results revealed the excellent potential of CuFC-MHBs for the treatment of cesium-contaminated sources resulted from nuclear accidents or radioactive liquid -waste. Also, Liu et al. [102] fabricated hydrogel microfibers by adding sodium alginate in the continuous phase to calcium ions to cross-link with it. A simple microfluidic technique was applied to produce water-in-water droplets encapsulated in fabricated hydrogel microfibers, which provided a shell matrix for manipulation to generate droplets easily. Bacillus subtilis loaded in droplets in hydrogel fiber showed nitrite-N removal capability for sewage and could be easily separated, illustrating the great potential of fiber format comprising aqueous microdroplets in bioreactor applications.

Ongoing to investigate the symbiosis hydrogel-based materials in ion adsorption and wastewater remediation, Qi et al. [103] investigated a polysaccharide-constructed hydrogel that presented a significant

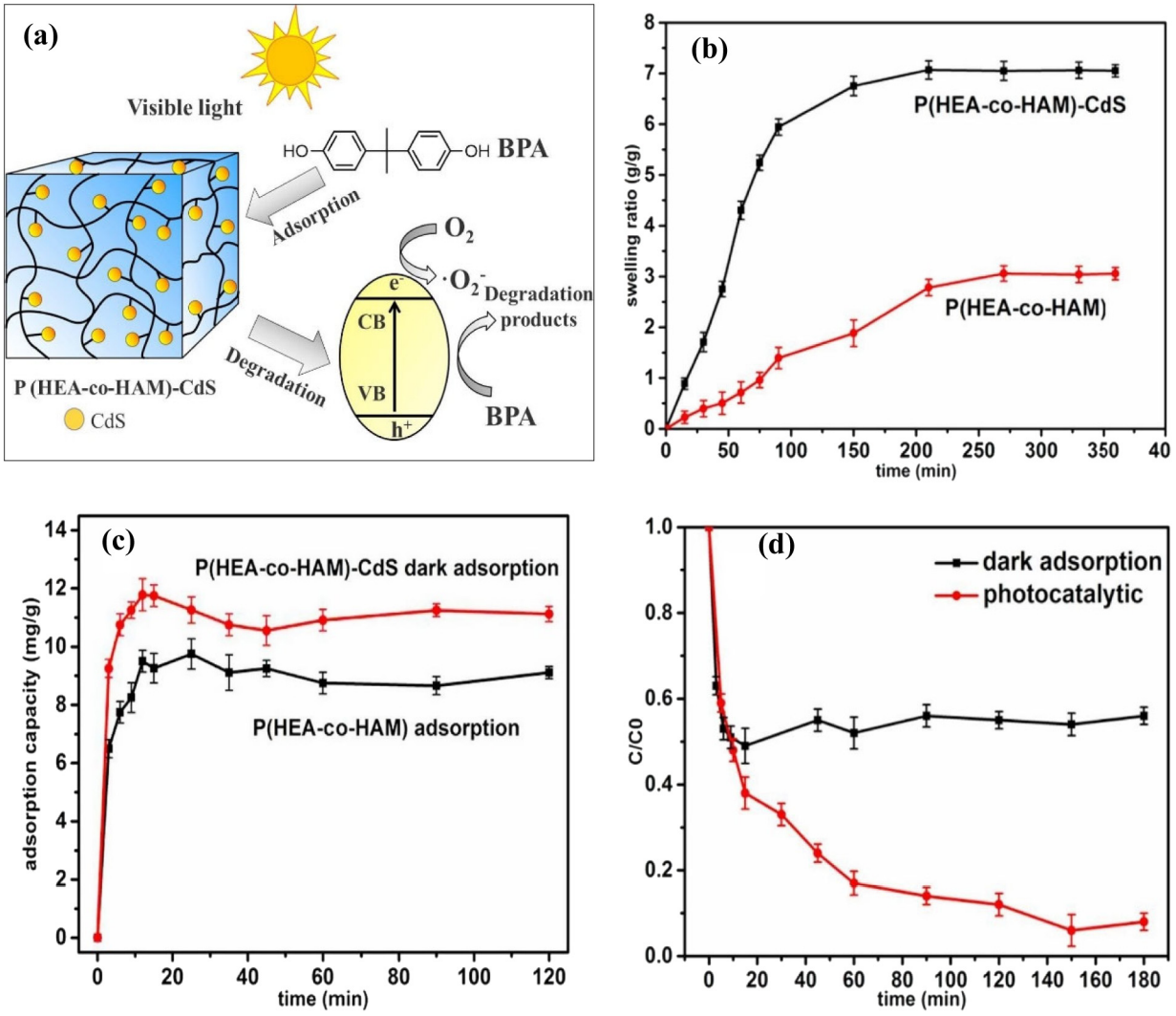

Fig. 10. (a) Schematic of process treatment, (b) swelling ratio of hydrogel material with and without CdS, (c) adsorption capacity of hydrogel material with and without CdS, (d) degradation rate, and adsorption rate of P(HEA-co-HAM)-CdS [55].

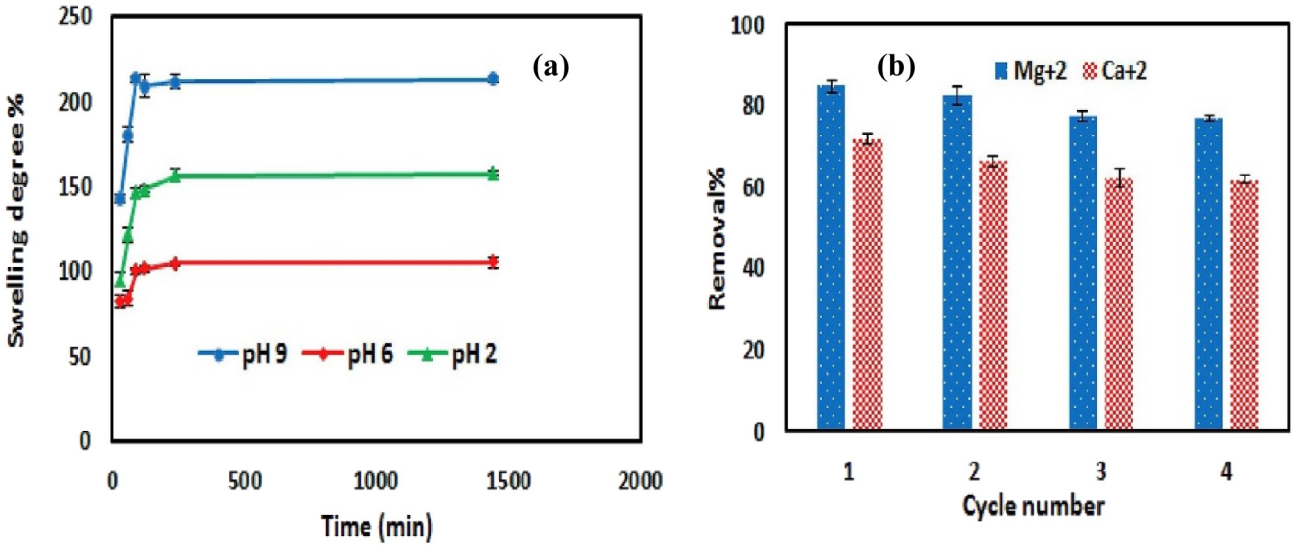

Fig. 11. (a) Variation of poly (AMPS)-g-GT swelling degree with respect to time under various pH values for water (b) variation of ions removal ability of poly (AMPS)-g-GT after every adsorption/desorption cycle [104].

Table 3
Summary for wastewater remediation and ions adsorption-based hydrogel materials.

References	Proposed materials	Applications
Zhu et al. [55]	P(HEA-co-HAM)-CdS	BPA removal from wastewater
Panao et al. [100]	Hybrid hydrogel based on alginate and SiO_2 microspheres	Methylene blue removal from wastewater
Lee et al. [101]	CuFC-MHBs	Cesium removal from water
Liu et al. [102]	Water-in-water droplets encapsulated in hyrogel microfibers based on sodium alginate and calcium ions	Nitrite-N removal from sewage
Qi et al. [103]	EPS-g-PSM	Chemical adsorption of Cu^{2+} from water
Mohammadian et al. [104]	Poly (AMPS)-g-GT	Adsorption of Ca^{2+} and Mg^{2+} from water

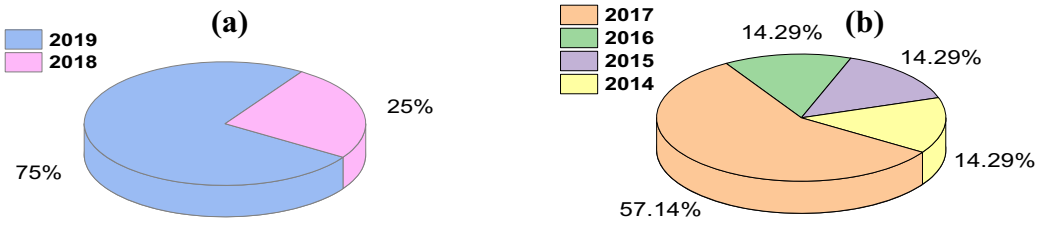

Fig. 12. Pie charts for the published work during the last six years concerning water evaporation. (a) Based on hydrogel, (b) based on other materials for heat localization.

Table 4
Comparison summary between the hydrogel-based evaporation and other materials in terms of mass change and efficiency.

Materials app. (under 1 sun illumination)	Mass change, kg m^{-2} h^{-}	Efficiency, %	References
a) Hydrogel-based evaporation			
Copper sulfide-microporous polyacrylamide hydrogel (CuSPH)	1.4	92	Sun et al. [76]
Silver nanoparticles (Ag NPs) and poly (sodium-p-styrene sulfonate) (PSS) decorated agarose gel (AG) (Ag + PSS + AG/AG)	2.1	92.8	Sun et al. [78]
Polyvinyl alcohol and solar Absorber (reduced graphene oxide) (PVA+ rGO)	2.5	95	Zhou et al. [79]
Silicon dioxide+polyvinyl alcohol with polypyrrole (SiO_2 + PVA + PPy)	1.8	82.2	Tan et al. [90]
Polyvinyl alcohol with polypyrrole (PVA + PPy)	3.6	92	Zhou et al. [85]
Polyvinyl alcohol with polypyrrole (PVA + PPy)	3.2	94	Zhao et al. [86]
Polyacrylamide+ Multi-Walled Carbon Nanotubes (PAAM+ MWCNT)	2	85.7	Xu et al. [80]
Double-network hydrogel (DNH)	1.4	91.5	Yin et al. [81]
Polyvinyl alcohol+ Titanium oxide (PVA+ Ti_2O_3)	3.6	90	Guo et al. [82]
Carbon dots + composite material comprising (C-dots + CMC)	1.4	89	Singh et al. [92]
Polyvinyl alcohol + activated carbon (PVA + AC)	2.6	91	Guo et al. [93]
Melamine foam with polypyrrole (MF + PPy)	1.5	90.4	Li et al. [89]
b) Other materials based evaporation			
Graphene foam (HGF)	1.4	91.4	Ren et al. [108]
Carbon black (BP)	1.28	88.2	Liu et al. [109]
Mushrooms (Mus)	1.27	78	Xu et al. [107]
Double-layer structure carbon foam and exfoliated graphite (DLG)	1	64	Ghasemi et al. [110]
Thin-film black gold membrane (TF-BGM)	0.67	47	Bae et al. [105]
Wood (W)	1.05	72	Xue et al. [106]
Aluminium-basedplasmonic structure (ALNP)	1	58	Zhou et al. [111]

absorption capability of Cu^{2+}. The proposed hydrogel adsorbent (EPS-g-PSM) was fabricated by graft polymerization of 3-sulfopropyl methacrylate potassium salt (SM) along the chains of extracellular polysaccharide salecan (EPS). EPS and PSM were selected as host and side chains of the hydrogel matrix, respectively. X-ray diffraction, SEM, FTIR spectroscopy, rheometry, and TGA were carried out to detect the physicochemical features of a proposed adsorbent. It was shown that the pore size, swelling, adsorption, and mechanical performance of the proposed hydrogel could be controlled by changing the EPS amount. In the presence of an initiator, Mohammadian et al. [104] performed a radical polymerization for monomer of 2-acrylamido-2-methyl-1-propane-sulfonic acid on macromolecular chains of Gum Tragacance (GT) to obtain poly (AMPS)-g-GT. Poly (AMPS)-g-GT was mixed to PVA, silver metal nanoparticles and graphene oxide (GO). Then, this mixture was gelled to get a new antibacterial hydrogel bead. The effect of varying the ratio of beads components on the swelling behavior of hydrogel was investigated under three different pH values (2, 6, and 9) for the solution. The swelling degrees of the best composition under different pH values and contact times are shown in Fig. 11(a). Also, in this work, the metal ions removal percentage for the hydrogel was investigated, in addition, Ca^{2+} and Mg^{2+} adsorption by the proposed hydrogel was studied, and results showed that its maximum adsorption for these ions is 114.18 mg g^{-1} and 162.46 mg g^{-1}, respectively. Moreover, it showed great reusability. As shown in Fig. 11(b), the removal ability of hydrogel beads after four adsorption/desorption cycles reduced by only 6%.

Wastewater remediation based hydrogel materials are viable and still in the infant stage of applications, and a few studies were conducted in this regard, such as biorefractory organic matter removals (BPA), industrial dyes (Methylene blue), metal adsorption and inorganic nitrate removals. Table 3 summarizes all wastewater remediation and ions adsorption-based hydrogel materials.

5. Comparison summary between hydrogel-based evaporation and other materials

Conventional water evaporation using solar radiation is considered as an inefficient process, where most of the energy is wasted without

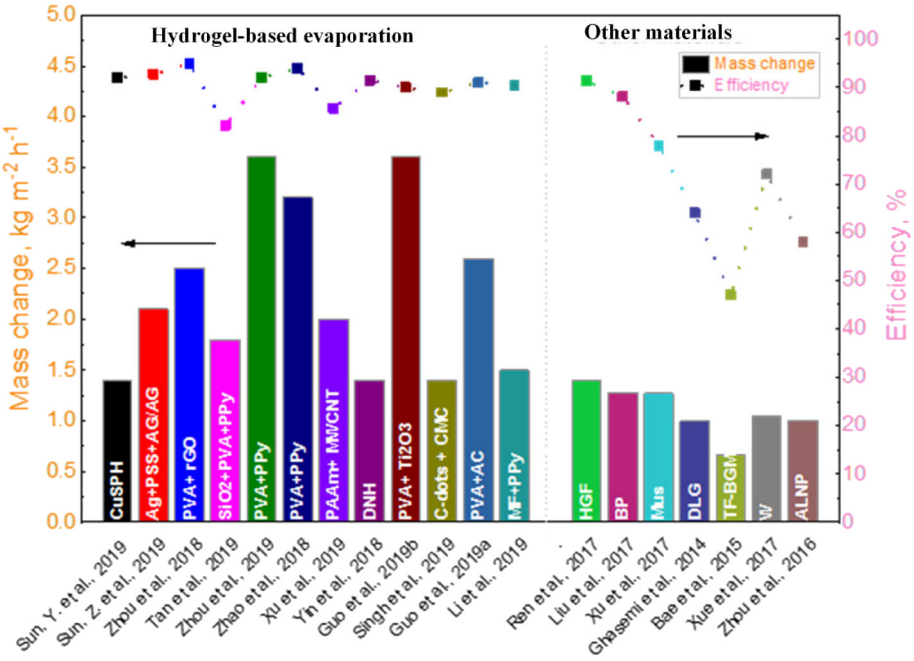

Fig. 13. Comparison between hydrogel-based evaporation and other materials in terms of mass change and efficiency.

useful usage. For instant, the average efficiency for conventional solar still systems is ranged from 30 to 40%. In contrast, applying hydrogel-based solar absorber in steam generation, water desalination, wastewater remediation, and cleaning industrial swage applications is one of the intelligent solutions to maximize the system efficiency (up to 95%) and improve its overall performance. This mainly attributed to the brilliant advantages of hydrogels materials such as high solar absorptivity, low heat losses, better energy confinement, excellent capillary action mechanisms, durability, cost-saving, etc.

Fig. 12 reveals the interest in different materials that have been applied for the evaporation process from 2014 to 2017, which are based on heat localization concept and without the integration of hydrogels materials. On the other hand, in the last two years, the efforts are directed to a new porous material (i.e., hydrogels), which showed a great increment in water evaporation rate and efficiency compared to other materials. It was founded that 75% of the published papers which are interested in hydrogel materials applications are in 2019, compared to only 25% in 2018.

In our summary, we selected some materials which gave an outstanding promotion in this process to show the numerical comparison between evaporation-based hydrogels and other materials. Table 4 and Fig. 13 summarize the efficiency and mass change under 1 sun illumination for previously discussed works, which applied various types of hydrogel for the water evaporation process. Also, a sample of other works applying other porous material, which has high-performance characteristics, are presented as well. For instance, Bae et al. [105] used a thin-film black gold membrane and reported an efficiency of 47% and a mass change of 0.67 kg m^{-2} h^{-1}. Organic materials are also used. As reported by Xue et al. [106] and Xu et al. [107], using wood and mushroom leads to an efficiency of 72 and 78%, and a mass change of 1.05 and 1.27 kg m^{-2} h^{-1}, respectively. Ren et al. [108] demonstrated that using graphene foam leads to an efficiency of 91.4% and a mass change of 1.4 kg m^{-2} h^{-1}. Moreover, Fig. 13 shows the obvious superiority of hydrogels, especially hybrid ones, over other porous materials with efficiency ranges between 82.2 and 95%, and mass change ranges between 1.4 and 3.6 kg m^{-2} h^{-1}.

6. Conclusion and recommendations for future work

Currently, the deficient of conventional solar evaporation systems inevitably brought scientists interest for substantial improvement and technological advancement in water purification and wastewater treatments. In this review, the intimate role of interfacial solar absorbers in water evaporation systems was evaluated. Obviously, incorporating solar absorbers in the solar steam generation process outperformed the current technologies, and higher clean water production was multiplied a dozen times. Various types hydrogels based solar absorber material were presented and evaluated, in which the hydrogel materials have great potential to improve photothermal interfacial evaporation systems, owing to its solar absorbance promotion, minimal heat losses, energy confinement features, mechanical stability properties, excellent capillary action mechanisms, scalability, durability and cost reduction benefits. Moreover, hydrogel-based catalyst materials can be used as an efficient treatment of highly contaminated wastewater for improving biodegradability removal efficiency.

However, hydrogel-based interfacial photothermal absorbance materials are currently limited to the laboratory experiments, and the gap between the current state-of-art and real field applications is considerable. Thus, from the engineering point of view, the outdoor application of photothermal technology needs more investigation to be a competitive alternative for the conventional solar steam technologies before its being be commercialized. Moreover, further studies should focus on the obstacles of current systems in parallel with the development of hydrogel materials, in which the existing water condensation and collection strategies are limiting the maximization of clean water production and significantly affect the whole system. In this regard, priority should also be given to the sustainability of drinking water applications, in which efficient and complementary photothermal engineering designs are needed for continuity and human beings.

As obviously noticed, the application of hydrogel materials in water applications are a new trend and still under research to affirm their superiority or inferiority compared to other indeed applied methods. In addition, there are a lot of challenges that require more investigations that can give advanced enhancements in this research area. For so, some suggestions are proposed for future work as follows:

- ➢ More attention toward the real-world applications of different hydrogel structures (with large scale) is required instead of lab experiments to quantify the tangible benefits of hydrogels.
- ➢ Cost estimation of 1 L of the produced freshwater using hydrogel materials should be intensively carried out.
- ➢ New types of hydrogel materials integrated with nanoparticles (organic and metallic) as a photothermal conversion should be developed.
- ➢ Further application of hybrid absorber materials should be investigated.
- ➢ Energy, exergy, economic, and environmental (4E) based analyses should be carried out to evaluate the feasibility of utilizing hydrogel materials in water evaporation and wastewater treatment applications.

Declaration of competing interest

The authors whose names are listed immediately below certify that they have NO affiliations with or involvement in any organization or entity with any financial interest (such as honoraria; educational grants; participation in speakers' bureaus; membership, employment, consultancies, stock ownership, or other equity interest; and expert testimony or patent-licensing arrangements), or non-financial interest (such as personal or professional relationships, affiliations, knowledge or beliefs) in the subject matter or materials discussed in this manuscript.

Acknowledgement

The work was sponsored by National Key Research and Development Program of China (2018YFE0127800), National Natural Science Foundation of China (51950410592) and Fundamental Research Funds for the Central Universities (2019kfyRCPY045). The authors thank the National Supercomputing Center in Tianjin (NSCC-TJ) and China Scientific Computing Grid (ScGrid) for providing assistance in computations.

References

[1] I. Haddeland, J. Heinke, H. Biemans, S. Eisner, M. Flörke, N. Hanasaki, M. Konzmann, F. Ludwig, Y. Masaki, J. Schewe, T. Stacke, Z.D. Tessler, Y. Wada, D. Wisser, Global Water Resources Affected by Human Interventions and Climate Change, Proc Natl Acad Sci U S A 111 (2014) 3251–3256.
[2] M.M. Mekonnen, A.Y. Hoekstra, Four Billion People Facing Severe Water Scarcity, Science Advances 2 (2016) e1500323.
[3] Y. Fu, G. Wang, X. Ming, X. Liu, B. Hou, T. Mei, J. Li, J. Wang, X. Wang, Oxygen plasma treated graphene aerogel as a solar absorber for rapid and efficient solar steam generation, Carbon 130 (2018) 250–256.
[4] G. Wang, Y. Fu, X. Ma, W. Pi, D. Liu, X. Wang, Reusable reduced graphene oxide based double-layer system modified by polyethylenimine for solar steam generation, Carbon 114 (2017) 117–124.
[5] T. Shichi, K. Takagi, Clay Minerals as Photochemical Reaction Fields, Journal of Photochemistry and Photobiology C: Photochemistry Reviews 1 (2000) 113–130.
[6] X. Huang, P.K. Jain, I.H. El-Sayed, M.A. El-Sayed, Plasmonic Photothermal Therapy (PPTT) Using Gold Nanoparticles, Lasers in Medical Science 23 (2008) 217.
[7] H.A. Atwater, A. Polman, Plasmonics for improved photovoltaic devices, Materials for Sustainable Energy: A Collection of Peer-reviewed Research and Review Articles From Nature Publishing Group, World Scientific, 2011, pp. 1–11.
[8] T.A. Yassen, N.D. Mokhlif, M.A. Eleiwi, Performance investigation of an integrated solar water heater with corrugated absorber surface for domestic use, Renew. Energy 138 (2019) 852–860.
[9] A.E. Kabeel, M.H. Hamed, Z.M. Omara, A.W. Kandeal, Solar air heaters: design configurations, improvement methods and applications – a detailed review, Renew. Sust. Energ. Rev. 70 (2017) 1189–1206.
[10] B. Bala, S. Janjai, Solar drying of fruits, vegetables, spices, medicinal plants and fish: developments and potentials, International Solar Food Processing Conference, 2009, pp. 14–16.
[11] N.S. Lewis, Research Opportunities to Advance Solar Energy Utilization, Science 351 (2016) aad1920.
[12] M.H. Khoshgoftar Manesh, H. Ghalami, M. Amidpour, M.H. Hamedi, Optimal coupling of site utility steam network with MED-RO desalination through total site analysis and exergoeconomic optimization, Desalination 316 (2013) 42–52.
[13] A. Farsi, I. Dincer, Development and evaluation of an integrated MED/membrane desalination system, Desalination 463 (2019) 55–68.
[14] W. El-Mudir, M. El-Bousiffi, S. Al-Hengari, Performance evaluation of a small size TVC desalination plant, Desalination 165 (2004) 269–279.
[15] M.H. Hamed, A.E. Kabeel, Z.M. Omara, S.W. Sharshir, Mathematical and experimental investigation of a solar humidification–dehumidification desalination unit, Desalination 358 (2015) 9–17.
[16] A.E. Kabeel, M.H. Hamed, Z.M. Omara, S.W. Sharshir, Experimental study of a humidification-dehumidification solar technique by natural and forced air circulation, Energy 68 (2014) 218–228.
[17] S.W. Sharshir, G. Peng, N. Yang, M.A. Eltawil, M.K.A. Ali, A.E. Kabeel, A hybrid desalination system using humidification-dehumidification and solar stills integrated with evacuated solar water heater, Energy Convers. Manag. 124 (2016) 287–296.
[18] S.W. Sharshir, M.O.A. El-Samadony, G. Peng, N. Yang, F.A. Essa, M.H. Hamed, A.E. Kabeel, Performance enhancement of wick solar still using rejected water from humidification-dehumidification unit and film cooling, Appl. Therm. Eng. 108 (2016) 1268–1278.
[19] S.W. Sharshir, G. Peng, N. Yang, M.O.A. El-Samadony, A.E. Kabeel, A continuous desalination system using humidification – dehumidification and a solar still with an evacuated solar water heater, Appl. Therm. Eng. 104 (2016) 734–742.
[20] A.D. Khawaji, I.K. Kutubkhanah, J.-M. Wie, Advances in Seawater Desalination Technologies, Desalination 221 (2008) 47–69.
[21] R. Semiat, Energy Issues in Desalination Processes, Environmental Science & Technology 42 (2008) 8193–8201.
[22] Q. Schiermeier, Purification with a pinch of salt: climate change, growing populations and political concerns are prompting governments and investors from California to China to take a fresh look at desalination, Quirin Schiermeier wades in, Nature 452 (2008) 260–262.
[23] S. Lattemann, T. Höpner, Environmental Impact and Impact Assessment of Seawater Desalination, Desalination 220 (2008) 1–15.
[24] M.R. Elkadeem, S. Wang, S.W. Sharshir, E.G. Atia, Feasibility analysis and techno-economic design of grid-isolated hybrid renewable energy system for electrification of agriculture and irrigation area: a case study in Dongola, Sudan, Energy Convers. Manag. 196 (2019) 1453–1478.
[25] O. Neumann, A.D. Neumann, E. Silva, C. Ayala-Orozco, S. Tian, P. Nordlander, N.J. Halas, Nanoparticle-mediated, Light-induced Phase Separations, Nano Lett. 15 (2015) 7880–7885.
[26] Y. Liu, J. Lou, M. Ni, C. Song, J. Wu, N.P. Dasgupta, P. Tao, W. Shang, T. Deng, Interfaces, Bioinspired Bifunctional Membrane for Efficient Clean Water Generation, ACS Appl. Mater. Interfaces 8 (2015) 772–779.
[27] B. Jiang, J. Zheng, S. Qiu, M. Wu, Q. Zhang, Z. Yan, Q. Xue, Review on Electrical Discharge Plasma Technology for Wastewater Remediation, Chem. Eng. J. 236 (2014) 348–368.
[28] C. Finnerty, L. Zhang, D.L. Sedlak, K.L. Nelson, B. Mi, Technology, Synthetic Graphene Oxide Leaf for Solar Desalination With Zero Liquid Discharge, Environmental Science & Technology 51 (2017) 11701–11709.
[29] G. Liu, J. Xu, K. Wang, Solar Water Evaporation by Black Photothermal Sheets, Nano Energy 41 (2017) 269–284.
[30] E. Chiavazzo, M. Morciano, F. Viglino, M. Fasano, P. Asinari, Passive Solar High-yield Seawater Desalination by Modular and Low-cost Distillation, Nature Sustainability 1 (2018) 763–772.
[31] Z. Deng, J. Zhou, L. Miao, C. Liu, Y. Peng, L. Sun, S. Tanemura, The Emergence of Solar Thermal Utilization: Solar-driven Steam Generation, Journal of Materials Chemistry A 5 (2017) 7691–7709.
[32] S.W. Sharshir, G. Peng, N. Yang, M.A. Eltawil, M.K.A. Ali, A. Kabeel, A hybrid desalination system using humidification-dehumidification and solar stills integrated with evacuated solar water heater, Energy Convers. Manag. 124 (2016) 287–296.
[33] S.W. Sharshir, G. Peng, L. Wu, F.A. Essa, A.E. Kabeel, N. Yang, The effects of flake graphite nanoparticles, phase change material, and film cooling on the solar still performance, Appl. Energy 191 (2017) 358–366.
[34] A.H. Elsheikh, S.W. Sharshir, M.E. Mostafa, F.A. Essa, M.K. Ahmed Ali, Applications of nanofluids in solar energy: a review of recent advances, Renew. Sust. Energ. Rev. 82 (2018) 3483–3502.
[35] S.W. Sharshir, G. Peng, A.H. Elsheikh, E.M.A. Edreis, M.A. Eltawil, T. Abdelhamid, A.E. Kabeel, J. Zang, N. Yang, Energy and exergy analysis of solar stills with micro/nano particles: a comparative study, Energy Convers. Manag. 177 (2018) 363–375.
[36] Y. Liu, S. Yu, R. Feng, A. Bernard, Y. Liu, Y. Zhang, H. Duan, W. Shang, P. Tao, C. Song, A Bioinspired, Reusable, Paper-based System for High-performance Large-scale Evaporation, Adv. Mater. 27 (2015) 2768–2774.
[37] L. Zhou, Y. Tan, J. Wang, W. Xu, Y. Yuan, W. Cai, S. Zhu, J. Zhu, 3D Self-assembly of Aluminium Nanoparticles for Plasmon-enhanced Solar Desalination, Nature Photonics 10 (2016) 393–398.
[38] C. Liu, J. Huang, C.E. Hsiung, Y. Tian, J. Wang, Y. Han, A. Fratalocchi, High-performance Large-scale Solar Steam Generation With Nanolayers of Reusable Biomimetic Nanoparticles, Advanced Sustainable Systems 1 (2017) 1600013.
[39] L. Zhang, B. Tang, J. Wu, R. Li, P. Wang, Hydrophobic Light-to-heat Conversion Membranes With Self-healing Ability for Interfacial Solar Heating, Advanced Materials 27 (2015) 4889–4894.
[40] P. Zhang, Q. Liao, T. Zhang, H. Cheng, Y. Huang, C. Yang, C. Li, L. Jiang, L. Qu, High Throughput of Clean Water Excluding Ions, Organic Media, and Bacteria From Defect-abundant Graphene Aerogel Under Sunlight, Nano Energy 46 (2018) 415–422.
[41] P. Yang, K. Liu, Q. Chen, J. Li, J. Duan, G. Xue, Z. Xu, W. Xie, J. Zhou, E. Science,

Solar-driven Simultaneous Steam Production and Electricity Generation From Salinity, Energy & Environmental Science 10 (2017) 1923–1927.
[42] H. Ren, M. Tang, B. Guan, K. Wang, J. Yang, F. Wang, M. Wang, J. Shan, Z. Chen, D. Wei, H. Peng, Z. Liu, Hierarchical Graphene Foam for Efficient Omnidirectional Solar–thermal Energy Conversion, Adv. Mater. 29 (2017) 1702590.
[43] G. Peng, H. Ding, S.W. Sharshir, X. Li, H. Liu, D. Ma, L. Wu, J. Zang, H. Liu, W. Yu, H. Xie, N. Yang, Low-cost high-efficiency solar steam generator by combining thin film evaporation and heat localization: both experimental and theoretical study, Appl. Therm. Eng. 143 (2018) 1079–1084.
[44] A.H. Elsheikh, S.W. Sharshir, M.K. Ahmed Ali, J. Shaibo, E.M.A. Edreis, T. Abdelhamid, C. Du, Z. Haiou, Thin film technology for solar steam generation: a new dawn, Sol. Energy 177 (2019) 561–575.
[45] C. Chen, Y. Li, J. Song, Z. Yang, Y. Kuang, E. Hitz, C. Jia, A. Gong, F. Jiang, J.Y. Zhu, B. Yang, J. Xie, L. Hu, Highly Flexible and Efficient Solar Steam Generation Device, Adv. Mater. 29 (2017) 1701756.
[46] N. Xu, X. Hu, W. Xu, X. Li, L. Zhou, S. Zhu, J. Zhu, Mushrooms as Efficient Solar Steam-generation Devices, Adv. Mater. 29 (1) (2017) 1606762.
[47] Y. Fu, G. Wang, X. Ming, X. Liu, B. Hou, T. Mei, J. Li, J. Wang, X. Wang, Oxygen Plasma Treated Graphene Aerogel as a Solar Absorber for Rapid and Efficient Solar Steam Generation, Carbon 130 (2018) 250–256.
[48] P. Mu, W. Bai, Z. Zhang, J. He, H. Sun, Z. Zhu, W. Liang, A. Li, Robust Aerogels Based on Conjugated Microporous Polymer Nanotubes With Exceptional Mechanical Strength for Efficient Solar Steam Generation, Journal of Materials Chemistry A 6 (2018) 18183–18190.
[49] F. Jiang, H. Liu, Y. Li, Y. Kuang, X. Xu, C. Chen, H. Huang, C. Jia, X. Zhao, E. Hitz, Interfaces, Lightweight, Mesoporous, and Highly Absorptive All-nanofiber Aerogel for Efficient Solar Steam Generation, ACS Appl. Mater. Interfaces 10 (2017) 1104–1112.
[50] D. Lapotko, Optical excitation and detection of vapor bubbles around plasmonic nanoparticles, Opt. Express 17 (2009) 2538–2556.
[51] O. Neumann, A.S. Urban, J. Day, S. Lal, P. Nordlander, N.J. Halas, Solar vapor generation enabled by nanoparticles, ACS Nano 7 (2012) 42–49.
[52] Y. Zeng, J. Yao, B.A. Horri, K. Wang, Y. Wu, D. Li, H. Wang, Solar Evaporation Enhancement Using Floating Light-absorbing Magnetic Particles, Energy & Environmental Science 4 (2011) 4074–4078.
[53] L. Rizzo, D. Sannino, V. Vaiano, O. Sacco, A. Scarpa, D. Pietrogiacomi, Effect of solar simulated N-doped TiO2 photocatalysis on the inactivation and antibiotic resistance of an E. coli strain in biologically treated urban wastewater, Appl. Catal. B Environ. 144 (2014) 369–378.
[54] Y. Liu, X. Wang, H. Wu, High-performance wastewater treatment based on reusable functional photo-absorbers, Chem. Eng. J. 309 (2017) 787–794.
[55] H. Zhu, Z. Li, J. Yang, A novel composite hydrogel for adsorption and photocatalytic degradation of bisphenol a by visible light irradiation, Chem. Eng. J. 334 (2018) 1679–1690.
[56] H. Ghasemi, G. Ni, A.M. Marconnet, J. Loomis, S. Yerci, N. Miljkovic, G. Chen, Solar Steam Generation by Heat Localization, Nat. Commun. 5 (2014) 4449.
[57] K. Kaur, R. Jindal, Comparative Study on the Behaviour of Chitosan-gelatin Based Hydrogel and Nanocomposite Ion Exchanger Synthesized Under Microwave Conditions Towards Photocatalytic Removal of Cationic Dyes, Carbohydrate Polymers 207 (2019) 398–410.
[58] Y.S. Zhang, A. Khademhosseini, Advances in engineering hydrogels, Science 356 (2017) eaaf3627.
[59] S.S. Lee, H.D. Kim, S.H.L. Kim, I. Kim, I.G. Kim, J.S. Choi, J. Jeong, J.H. Kim, S.K. Kwon, N.S. Hwang, Self-healing and adhesive artificial tissue implant for voice recovery, ACS Applied Bio Materials 1 (2018) 1134–1146.
[60] E. Larson, R. Girard, C.L. Pessoa-Silva, J. Boyce, L. Donaldson, D. Pittet, Skin reactions related to hand hygiene and selection of hand hygiene products, Am. J. Infect. Control 34 (2006) 627–635.
[61] A. Childs, H. Li, D.M. Lewittes, B. Dong, W. Liu, X. Shu, C. Sun, H.F. Zhang, Fabricating Customized Hydrogel Contact Lens, Scientific Reports 6 (2016) 1–6.
[62] S. Singh, A. Mishra, R. Kumari, K.K. Sinha, M.K. Singh, P. Das, Carbon Dots Assisted Formation of DNA Hydrogel for Sustained Release of Drug, Carbon 114 (2017) 169–176.
[63] D. Cheng, Y. Liu, G. Yang, A. Zhang, Water- and fertilizer-integrated hydrogel derived from the polymerization of acrylic acid and urea as a slow-release N fertilizer and water retention in agriculture, J. Agric. Food Chem. 66 (2018) 5762–5769.
[64] I. Willner, Stimuli-controlled hydrogels and their applications, Acc. Chem. Res. 50 (2017) 657–658.
[65] J. Kopecek, Hydrogel biomaterials: a smart future? Biomaterials 28 (2007) 5185–5192.
[66] Y. Sun, J. Gao, Y. Liu, H. Kang, M. Xie, F. Wu, H. Qiu, Copper Sulfide-macroporous Polyacrylamide Hydrogel for Solar Steam Generation, Chemical Engineering Science 207 (2019) 516–526.
[67] L. Zhao, P. Wang, J. Tian, J. Wang, L. Li, L. Xu, Y. Wang, X. Fei, Y. Li, A Novel Composite Hydrogel for Solar Evaporation Enhancement at Air-Water, Interface,Sci Total Environ 668 (2019) 153–160.
[68] Z. Sun, J. Wang, Q. Wu, Z. Wang, Z. Wang, J. Sun, C.J. Liu, Plasmon Based Double-Layer Hydrogel Device for a Highly Efficient Solar Vapor Generation, Advanced Functional Materials 29 (2019) 1901312.
[69] J. Höpfner, T. Richter, P. Košovan, C. Holm, M. Wilhelm, Seawater desalination via hydrogels: practical realisation and first coarse grained simulations, Springer International Publishing, Cham, 2013, pp. 247–263.
[70] X. Zhou, F. Zhao, Y. Guo, Y. Zhang, G. Yu, A Hydrogel-based Antifouling Solar Evaporator for Highly Efficient Water Desalination, Energy & Environmental Science 11 (2018) 1985–1985–1992..
[71] H. Jin, G. Lin, L. Bai, A. Zeiny, D. Wen, Steam Generation in a Nanoparticle-based Solar Receiver, Nano Energy 28 (2016) 397–406.
[72] Z. Li, T. Chen, S. Liu, M. Zhao, K. Chen, D. Chen, J. Chen, Large-scale Pattern Fabrication of 3D rGO-Ag@ Ag3PO4 Hydrogel Composite Photocatalyst With the Excellent Synergistic Effect of Adsorption and Photocatalysis Degradation, Catalysis Today (2018).
[73] Q. Hao, T. Chen, R. Wang, J. Feng, D. Chen, W. Yao, A Separation-free Polyacrylamide/Bentonite/Graphitic Carbon Nitride Hydrogel With Excellent Performance in Water Treatment, Journal of Cleaner Production 197 (2018) 1222–1230.
[74] M. Lučić, N. Milosavljević, M. Radetić, Z. Šaponjić, M. Radoičić, M.K. Krušić, The Potential Application of TiO2/Hydrogel Nanocomposite for Removal of Various Textile Azo Dyes, Separation and Purification Technology 122 (2014) 206–216.
[75] Y. Hu, Z. Li, J. Yang, H. Zhu, Degradation of Methylparaben Using BiOI-hydrogel Composites Activated Peroxymonosulfate Under Visible Light Irradiation, Chem. Eng. Sci. 360 (2019) 200–211.
[76] Y. Sun, J. Gao, Y. Liu, H. Kang, M. Xie, F. Wu, H. Qiu, Copper sulfide-macroporous polyacrylamide hydrogel for solar steam generation, Chem. Eng. Sci. 207 (2019) 516–526.
[77] L. Zhao, P. Wang, J. Tian, J. Wang, L. Li, L. Xu, Y. Wang, X. Fei, Y. Li, A novel composite hydrogel for solar evaporation enhancement at air-water interface, Sci. Total Environ. 668 (2019) 153–160.
[78] Z. Sun, J. Wang, Q. Wu, Z. Wang, Z. Wang, J. Sun, C.J. Liu, Plasmon based double-layer hydrogel device for a highly efficient solar vapor generation, Adv. Funct. Mater. 29 (2019) 1901312.
[79] X. Zhou, F. Zhao, Y. Guo, Y. Zhang, G. Yu, A hydrogel-based antifouling solar evaporator for highly efficient water desalination, Energy Environ. Sci. 11 (2018) 1985–1992.
[80] W. Xu, Y. Xing, J. Liu, H. Wu, Y. Cui, D. Li, D. Guo, C. Li, A. Liu, H. Bai, Efficient water transport and solar steam generation via radially, hierarchically structured aerogels, ACS Nano 13 (2019) 7930–7938.
[81] X. Yin, Y. Zhang, Q. Guo, X. Cai, J. Xiao, Z. Ding, J. Yang, Macroporous double-network hydrogel for high-efficiency solar steam generation under 1 sun illumination, ACS Appl. Mater. Interfaces 10 (2018) 10998–11007.
[82] Y. Guo, X. Zhou, F. Zhao, J. Bae, B. Rosenberger, G. Yu, Synergistic energy nanoconfinement and water activation in hydrogels for efficient solar water desalination, ACS Nano 13 (2019) 7913–7919.
[83] Z. Deng, L. Miao, P.-F. Liu, J. Zhou, P. Wang, Y. Gu, X. Wang, H. Cai, L. Sun, S. Tanemura, Extremely high water-production created by a nanoink-stained PVA evaporator with embossment structure, Nano Energy 55 (2019) 368–376.
[84] P.-F. Liu, L. Miao, Z. Deng, J. Zhou, H. Su, L. Sun, S. Tanemura, W. Cao, F. Jiang, L.-D. Zhao, A mimetic transpiration system for record high conversion efficiency in solar steam generator under one-sun, Materials Today Energy 8 (2018) 166–173.
[85] X. Zhou, F. Zhao, Y. Guo, B. Rosenberger, G. Yu, Architecting highly hydratable polymer networks to tune the water state for solar water purification, Sci. Adv. 5 (2019) eaaw5484.
[86] F. Zhao, X. Zhou, Y. Shi, X. Qian, M. Alexander, X. Zhao, S. Mendez, R. Yang, L. Qu, G. Yu, Highly efficient solar vapour generation via hierarchically nanostructured gels, Nat. Nanotechnol. 13 (2018) 489–495.
[87] F. Ni, P. Xiao, C. Zhang, Y. Liang, J. Gu, L. Zhang, T. Chen, Micro-/macroscopically synergetic control of switchable 2D/3D photothermal water purification enabled by robust, portable, and cost-effective cellulose papers, ACS Appl. Mater. Interfaces 11 (2019) 15498–15506.
[88] W. Wang, J. Niu, J. Guo, L. Yin, H. Huang, In situ synthesis of PPy-FexOy-CTS nanostructured gel membrane for highly efficient solar steam generation, Sol. Energy Mater. Sol. Cells 201 (2019) 110046.
[89] C. Li, D. Jiang, B. Huo, M. Ding, C. Huang, D. Jia, H. Li, C.-Y. Liu, J. Liu, Scalable and robust bilayer polymer foams for highly efficient and stable solar desalination, Nano Energy 60 (2019) 841–849.
[90] M. Tan, J. Wang, W. Song, J. Fang, X. Zhang, Self-floating hybrid hydrogels assembled with conducting polymer hollow spheres and silica aerogel microparticles for solar steam generation, J. Mater. Chem. A 7 (2019) 1244–1251.
[91] H. Su, J. Zhou, L. Miao, J. Shi, Y. Gu, P. Wang, Y. Tian, X. Mu, A. Wei, L. Huang, S. Chen, Z. Deng, A hybrid hydrogel with protonated g-C3N4 and graphene oxide as an efficient absorber for solar steam evaporation, Sustain. Mater. Technol. 20 (2019) e00095.
[92] S. Singh, N. Shauloff, R. Jelinek, Solar-enabled water remediation via recyclable carbon dot/hydrogel composites, ACS Sustain. Chem. Eng. 7 (2019) 13186–13194.
[93] Y. Guo, F. Zhao, X. Zhou, Z. Chen, G. Yu, Tailoring nanoscale surface topography of hydrogel for efficient solar vapor generation, Nano Lett. 19 (2019) 2530–2536.
[94] R. Li, Y. Shi, M. Alsaedi, M. Wu, L. Shi, P. Wang, Hybrid hydrogel with high water vapor harvesting capacity for deployable solar-driven atmospheric water generator, Environmental Science & Technology 52 (2018) 11367–11377.
[95] T. Wang, Z. Dai, J. Kang, F. Fu, T. Zhang, S. Wang, A TiO 2 nanocomposite hydrogel for hydroponic plants in efficient water improvement, Mater. Chem. Phys. 215 (2018) 242–250.
[96] J. Zeng, S. Cui, Q. Wang, R. Chen, Multi-layer temperature-responsive hydrogel for forward-osmosis desalination with high permeable flux and fast water release, Desalination 459 (2019) 105–113.
[97] T. Yamamoto, A. Yasuhara, H. Shiraishi, O. Nakasugi, Bisphenol a in hazardous waste landfill leachates, Chemosphere 42 (2001) 415–418.
[98] J. Sharma, I.M. Mishra, D.D. Dionysiou, V. Kumar, Oxidative removal of bisphenol A by UV-C/peroxymonosulfate (PMS): kinetics, influence of co-existing chemicals and degradation pathway, Chem. Eng. J. 276 (2015) 193–204.
[99] L. Zhao, Y. Ji, D. Kong, J. Lu, Q. Zhou, X. Yin, Simultaneous removal of bisphenol A and phosphate in zero-valent iron activated persulfate oxidation process, Chem.

Eng. J. 303 (2016) 458–466.
[100] C.O. Panão, E.L.S. Campos, H.H.C. Lima, A.W. Rinaldi, M.K. Lima-Tenório, E.T. Tenório-Neto, M.R. Guilherme, T. Asefa, A.F. Rubira, Ultra-absorbent hybrid hydrogel based on alginate and SiO2 microspheres: a high-water-content system for removal of methylene blue, J. Mol. Liq. 276 (2019) 204–213.
[101] I. Lee, C.W. Park, S.S. Yoon, H.M. Yang, Facile synthesis of copper ferrocyanide-embedded magnetic hydrogel beads for the enhanced removal of cesium from water, Chemosphere 224 (2019) 776–785.
[102] C. Liu, W. Zheng, R. Xie, Y. Liu, Z. Liang, G. Luo, M. Ding, Q. Liang, Microfluidic fabrication of water-in-water droplets encapsulated in hydrogel microfibers, Chin. Chem. Lett. 30 (2019) 457–460.
[103] X. Qi, R. Liu, M. Chen, Z. Li, T. Qin, Y. Qian, S. Zhao, M. Liu, Q. Zeng, J. Shen, Removal of copper ions from water using polysaccharide-constructed hydrogels, Carbohydr. Polym. 209 (2019) 101–110.
[104] M. Mohammadian, R. Sahraei, M. Ghaemy, Synthesis and fabrication of anti-bacterial hydrogel beads based on modified-gum tragacanth/poly(vinyl alcohol)/Ag(0) highly efficient sorbent for hard water softening, Chemosphere 225 (2019) 259–269.
[105] K. Bae, G. Kang, S.K. Cho, W. Park, K. Kim, W.J. Padilla, Flexible thin-film black gold membranes with ultrabroadband plasmonic nanofocusing for efficient solar vapour generation, Nat. Commun. 6 (2015) 10103.
[106] G. Xue, K. Liu, Q. Chen, P. Yang, J. Li, T. Ding, J. Duan, B. Qi, J. Zhou, Robust and low-cost flame-treated wood for high-performance solar steam generation, ACS Appl. Mater. Interfaces 9 (2017) 15052–15057.
[107] N. Xu, X. Hu, W. Xu, X. Li, L. Zhou, S. Zhu, J. Zhu, Mushrooms as efficient solar steam-generation devices, Adv. Mater. 29 (2017) 1606762.
[108] H. Ren, M. Tang, B. Guan, K. Wang, J. Yang, F. Wang, M. Wang, J. Shan, Z. Chen, D. Wei, Hierarchical graphene foam for efficient omnidirectional solar–thermal energy conversion, Adv. Mater. 29 (2017) 1702590.
[109] Z. Liu, H. Song, D. Ji, C. Li, A. Cheney, Y. Liu, N. Zhang, X. Zeng, B. Chen, J. Gao, Extremely cost-effective and efficient solar vapor generation under non-concentrated illumination using thermally isolated black paper, Global Chall. 1 (2017) 1600003.
[110] H. Ghasemi, G. Ni, A.M. Marconnet, J. Loomis, S. Yerci, N. Miljkovic, G. Chen, Solar steam generation by heat localization, Nat. Commun. 5 (2014) ncomms5449.
[111] L. Zhou, Y. Tan, J. Wang, W. Xu, Y. Yuan, W. Cai, S. Zhu, J. Zhu, 3D self-assembly of aluminium nanoparticles for plasmon-enhanced solar desalination, Nat. Photonics 10 (2016) 393–398.